Chinese Chemical Letters 34 (2023) 108300

Contents lists available at ScienceDirect

Chinese Chemical Letters

journal homepage: www.elsevier.com/locate/cclet

Nanoplatform-based cellular reactive oxygen species regulation for enhanced oncotherapy and tumor resistance alleviation

Meifang Wang, Ping'an Ma*, Jun Lin*

State Key Laboratory of Rare Earth Resource Utilization, Changchun Institute of Applied Chemistry, Chinese Academy of Sciences, Changchun 130022, China

ARTICLE INFO

Article history:
Received 8 November 2022
Revised 31 December 2022
Accepted 2 March 2023
Available online 10 March 2023

Keywords:
Nanoagents
ROS regulation
ROS-mediated cancer therapy
Multidrug resistance
Thermoresistance

ABSTRACT

The cancer cells realize their proliferation and metastasis activities based on the special redox adaptation to increased reactive oxygen species (ROS) level, which inversely makes them sensitive to external interference with their redox state. In view of this, in recent decades, researchers have made great efforts to construct a series of novel nanoplatform-based ROS-mediated cancer therapies through increasing ROS generation and inhibiting the ROS elimination. Besides, the multidrug resistance and thermoresistance of tumor are closely related to tumor redox state. Recently, numerous works have shown that ROS regulation in cancer cells can intervene in the expression, function and stability of related proteins to achieve reversal of tumor resistance. In this review, the recent researches about ROS-regulating nanoagents on cancer therapy and tumor resistance alleviation have been well summarized. Finally, the challenges and research directions of ROS-regulating nanoagents for future clinical translation are also discussed.

1. Introduction

Oxidative stress (OS) is the consequence of imbalance between excess oxidants and insufficient antioxidants, finally inducing the cancer death [1–3]. Reactive oxygen species (ROS), as the general term of oxygen-containing reactive chemical species, are the most important oxidants in cancer cells and responsible for cellular OS at high concentration [4–6]. In the past decades, great efforts have been made to increase the level of ROS in cancer cells to achieve the final antitumor purpose [7–10]. And a series of novel ROS-mediated therapies have emerged, such as photodynamic therapy (PDT) [11–13], sonodynamic therapy (SDT) [14–16], chemodynamic therapy (CDT) [17–19], enzyme dynamic therapy (EDT) [20–22], gas therapy [23–25]. In addition, elimination of high-level antioxidants in cancer cells has been proved to improve the efficacy of ROS as well as accelerate the redox imbalance toward OS [26–28].

Multidrug resistance (MDR) and thermoresistance are the two common types of tumor resistance. Cancer cells with the trait of MDR can simultaneously resistant to different drugs, which are capable to elude chemo-drugs and survive from the chemotherapy [29–31]. Different with MDR, thermoresistance is the natural cell self-preservation pathways under thermal stimulation. Heating on tumor sites to achieve tumors ablation is the classical process of hyperthermia therapy (HTT) [32–34]. However, the rapidly repairing of fever-type cell damages can greatly compromise the effects of HTT [35–37], especially low temperature HTT (less than 45 °C) [38]. ROS are essential for biological functions of cells, involving the modification and activation of proteins, transcription factors and genes [39]. Therefore, rational regulation of cellular ROS is a potential way to alleviate tumor resistance.

In this review, recent developments of nanoplatform-based cellular ROS regulation for ROS-mediated cancer therapy and tumor resistance alleviation will be summarized (Fig. 1). On one hand, the ROS regulation approaches based on the nanoagents for cancer therapy, including increasing ROS generation and inhibiting the ROS elimination, and the involved active substances will be overviewed. On the other hand, the cellular mechanisms of MDR and thermoresistance, as well as the recent researches of tumor resistance reversal based on ROS-regulating nanoagents will also be summarized. For the better understanding of ROS effect in the synergistic antitumor, redox regulatory of cancer cells will be briefly mentioned before the main topics. At last, some perspectives about the challenges and research directions of nanoplatform-based ROS-mediated synergistic cancer therapy will also be discussed.

2. Redox regulatory of cancer cells

2.1. Cellular redox homeostasis

In living organisms, ROS are normally generated for regulating the various physiological metabolism [40]. The original source of

* Corresponding authors.
E-mail addresses: mapa675@ciac.ac.cn (P. Ma), jlin@ciac.ac.cn (J. Lin).

https://doi.org/10.1016/j.cclet.2023.108300
1001-8417/

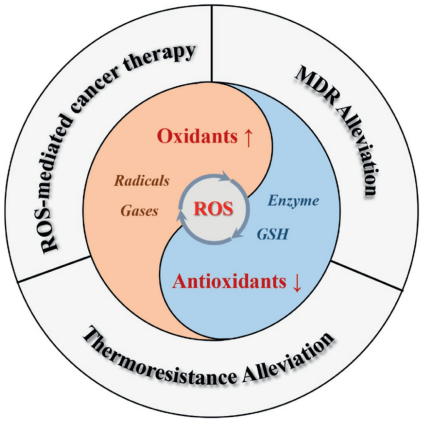

Fig. 1. Schematic illustration of nanoplatform-based ROS regulation and its application for cancer therapy and tumor resistance alleviation.

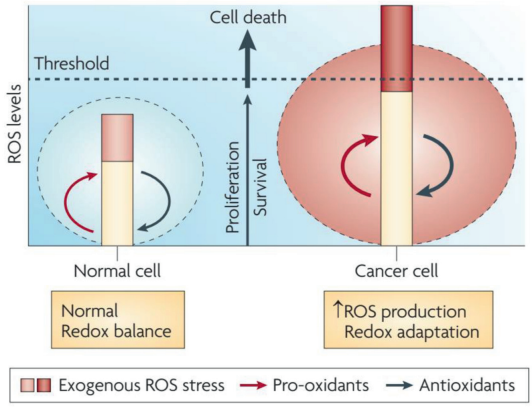

Fig. 3. Redox adaptation of normal cell and cancer cell. Reproduced with permission [56]. Copyright 2009, Nature Publishing Group.

most cellular ROS is O_2. Most of the molecular oxygen is consumed by mitochondria to maintain cellular energy metabolism, only a few parts of oxygen can be converted into ROS *via* mitochondrial respiratory chain (Mito-ETC), endoplasmic reticulum system (ER) and the NADPH oxidase complex (NOX) (Fig. 2) [41–43]. In a typical ROS generation process, molecular oxygen can capture the escaping electrons from electron transport chain in the mitochondria and be reduced into superoxide ($^{\bullet}O_2^-$) [44]. And subsequently, the $^{\bullet}O_2^-$ can be rapidly converted into H_2O_2 by superoxide dismutases (SOD) [45], and then H_2O_2 would be further turned into hydroxyl radicals ($^{\bullet}OH$) in the presence of Fe^{2+} [46]. Besides, the NO produced from arginine by NO synthase (NOS), can easily react with $^{\bullet}O_2^-$ to form peroxynitrite ($ONOO^-$) with higher reactivity for further modification and functionalization of proteins [47]. In another aspect, the ROS-scavenging systems including SOD, catalase (CAT) and glutathione (GSH), *etc.*, can effectively reduce the toxic ROS into non-toxic H_2O or others [48]. They would be activated once the ROS is excessive, finally realizing the cellular redox balance.

2.2. Redox adaptation of cancer cells

Malignant cells show higher levels of endogenous ROS than normal cells because of metabolic abnormalities and oncogenic signalling, which has been observed in freshly isolated leukaemia cells, clinical tumor specimens, plasma and so on [49–51]. Normally, irreversible oxidative damage would be induced under a severe increase of ROS level in cells, and followed by cell death. However, the cancer cells cannot only survive with the increased

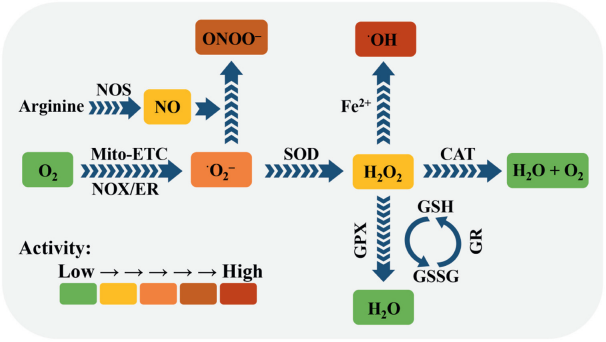

Fig. 2. Redox homeostasis of cancer cells. Mito-ETC, mitochondrial electron transport chain; NOX, NADPH oxidase complex; ER, endoplasmic reticulum system; NOS, nitric oxide synthase; SOD, superoxide dismutase; CAT, catalase; GPX, glutathione peroxidase; GR, glutathione reductase. The activity comparison refers to [40].

ROS stress, but also be promoted with the proliferation, immortalization, angiogenesis and metastasis [52–55]. This can be owing to the special redox adaptation of cancer cells, which is a kind of intense balance that involves high levels of ROS and high levels of antioxidants (Fig. 3) [56]. Different with cancer cells, the redox homeostasis in normal cells is based on the comfortable balance between a low level of basal ROS generation and elimination, far from the threshold. Therefore, the cancer cells are much more sensitive to the exogenous ROS than the normal cells, which could be applied as the basis to selectively kill cancer cells.

3. ROS regulation for cancer therapy

According to the previous reports, cancer cells have an evolved redox adaptation to promote their survival. In order to effectively kill the cancer cells, it is critical to manipulate and break the redox balance [57]. Since the cancer cells are the sensitive to exogenous ROS and over-dependent on the antioxidant system, increasing the ROS generation or inhibiting the ROS elimination are the two feasible strategies for realizing OS and cell death. In addition, the representative examples covered in this section are summarized and shown in Table 1.

3.1. Increasing the ROS generation

3.1.1. Classical radicals

Directly adding the excess oxidants is the most efficient way to increase the ROS level above the safe threshold. Exogenous radical $^1O_2$ is frequently used because of its high oxidation towards electron-rich organic molecules, such as proteins, nucleic acids and lipids, thus induce cell apoptosis [58]. Most production of $^1O_2$ requires oxygen consumption, for example, SDT [59] and PDT (type-II) [60], which would be limited in the hypoxia tumor microenvironment (TME).

Extra oxygen delivery *via* nanoliposomes [61], hemoglobin (Hb) [62], porous materials [63] *etc.* in the tumor site can significantly increase the ROS production of the photosensitizer or sonosensitizer. Considering that Hb is also abundant with natural metalloporphyrin, our group first attempted to apply Hb as a sonosensitizer for SDT (Fig. 4a) [64]. In addition, as a natural oxygen carrier, Hb can achieve the enhanced SDT effect by self-carrying oxygen. To enhance the stability and uptake ability of Hb, ZIF-8 was introduced as the carrier to realize pH-responsive Hb/O_2 release at tumor sites. Upon US irradiation, the as-prepared O_2@Hb@ZIF-8 (OHZ) can inhibit the growth of tumor cells through ROS-activated mitochondrial apoptosis pathway. Besides, catalyzing the decomposition of endogenous H_2O_2 by enzyme (natural enzyme CAT

Table 1
Representative examples of nanoplatforms based ROS regulation for cancer therapy.

Nanoplatforms	Type of ROS regulation	ROS-mediated therapy types	Section in text	Ref.
O_2@Hb@ZIF-8	Radicals ($^1O_2$)	SDT	3.1.1	[64]
OxgeMCC-r SAzyme	Radicals ($^1O_2$)	PDT	3.1.1	[70]
(MSNs@CaO_2-ICG)@LA	Radicals ($^1O_2$)	PDT	3.1.1	[73]
DCC-HA	Radicals ($^1O_2$)	EDT	3.1.1	[74]
CuO_2 nanodots	Radicals ($^{\bullet}OH$)	CDT	3.1.1	[83]
CaO_2-CuO_2@HA NC	Radicals ($^{\bullet}OH$)	CDT	3.1.1	[84]
BMT@LA NC	Gases (NO)/Radicals ($^1O_2$)	Gas therapy/SDT	3.1.2	[89]
PPOSD	Gases (CO)	Gas therapy	3.1.2	[95]
RUCSNs-DM	Gases (SO_2)	Gas therapy	3.1.2	[97]
$PdH_{0.2}$	Gases (H_2)	Gas therapy	3.1.2	[102]
2-ME/TK-CPT@ZIF-90@C	Inhibiting SOD	Chemotherapy	3.2.1	[103]
FeS@BSA	Inhibiting CAT/Radicals ($^{\bullet}OH$)	Gas therapy/CDT	3.2.1	[108]
CA/ALN@FcB	GSH depletion	Chemotherapy	3.2.2	[116]
$CaNP_{CAT+BSO}$@Ce6-PEG NPsPtH@FeP	GSH depletion/Radicals ($^1O_2$)	Chemotherapy/PDT	3.2.2	[117]
	GSH depletion/Radicals ($^{\bullet}OH$)	CDT	3.2.2	[118]
ICG loaded Cu-based MOF	GSH depletion/Radicals ($^{\bullet}OH$)	CDT	3.2.2	[119]
CMS@GOx	GSH depletion/Radicals ($^{\bullet}OH$, $^{\bullet}O_2^-$)	CDT/PDT	3.2.2	[120]
MnO_x-OVA/TF	GSH depletion/Radicals ($^{\bullet}OH$)	CDT	3.2.2	[121]
CuMOF@Pt(IV)	GSH depletion/Radicals ($^{\bullet}OH$)	Chemotherapy/CDT	3.2.2	[123]
GBMO	GSH depletion/Radicals ($^{\bullet}O_2^-$, $^1O_2$, $^{\bullet}OH$)	GSH-enhanced SDT	3.2.2	[126]
$SnS_{1.68}$-$WO_{2.41}$	GSH depletion/Gases (H_2)	GSH-enhanced gas therapy	3.2.2	[127]

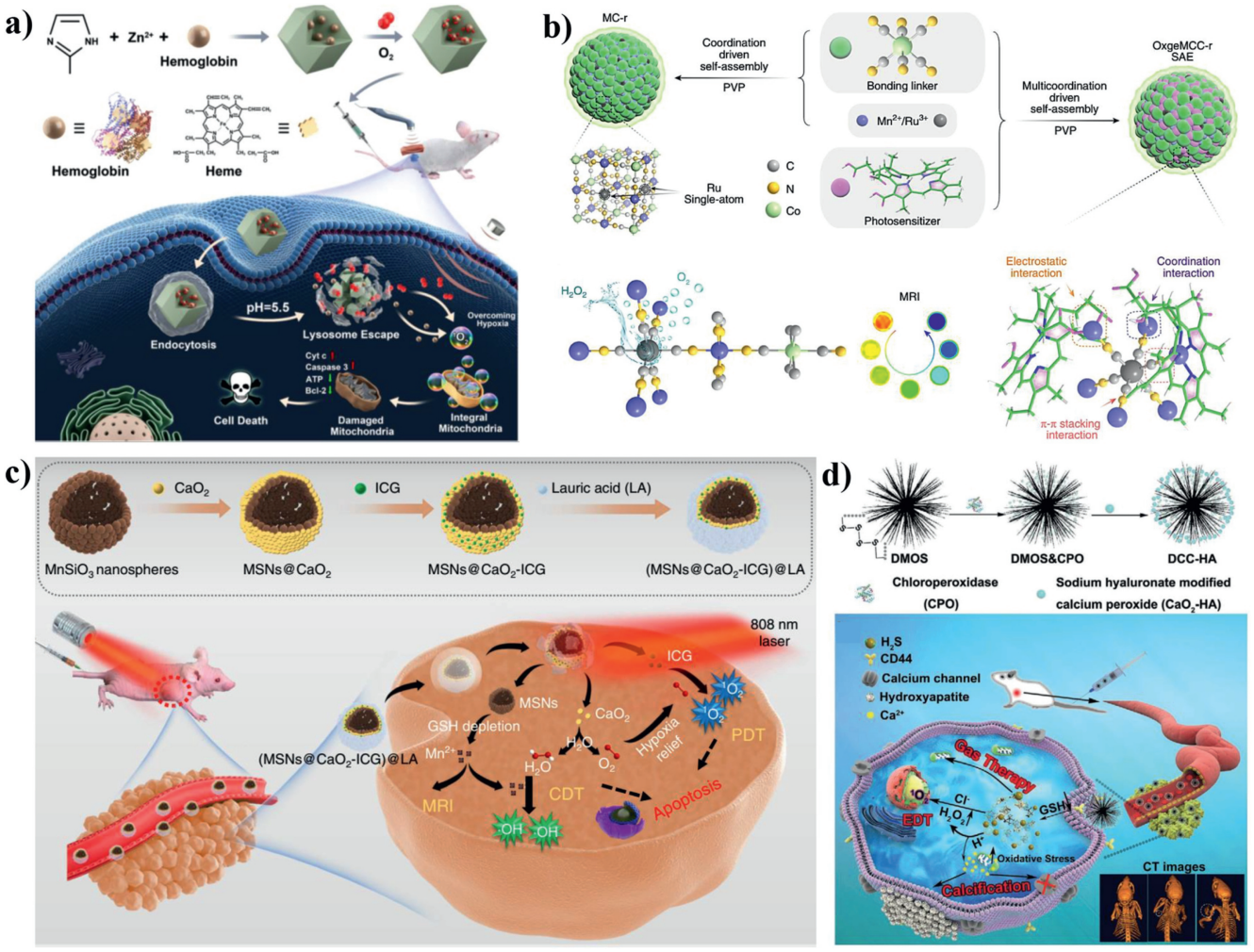

Fig. 4. (a) Schematic illustration of the synthesis and antitumor mechanism of OHZ nanoparticles. Reproduced with permission [64]. Copyright 2021, American Chemical Society. (b) Schematic illustration of OxgeMCC-r and its catalase-like performance. Reproduced with permission [70]. Copyright 2020, Nature Publishing Group. (c) The scheme of fabrication process and therapeutic mechanism of (MSNs@CaO2-ICG)@LA. Reproduced with permission [72]. Copyright 2020, Nature Publishing Group. (d) Schematic illustration of the synthesis and antitumor performance of the DCC-HA. Reproduced with permission [74]. Copyright 2021, Wiley-VCH.

[65] or nanozymes such as MnO_2 [66], Pt [67], single-atom enzyme (SAzyme) [68], *etc*.) is another feasible approach to increase the tumoral concentration of oxygen. The single-atom enzymes with highest atom utilization and abundant active sites offered new breakthroughs in cost-effective catalysis [69]. Recently, Zhao's group (Fig. 4b) reported a new type of single-atom ruthenium, OxgeMCC-r SAzyme, serving as a CAT-like nanozyme for oxygen generation to enhance the PDT efficacy of chlorin e6 (Ce6) [70]. According to authors, the six unsaturated Ru-C_6 coordination sites are responsible for the high catalytic activity of the OxgeMCC-r SAzyme.

The oxygen production from decomposition of H_2O_2 is more stable and specific than oxygen delivery, whereas the limited level (less than 100 μmol/L) of H_2O_2 [71] cannot support the enough O_2. In view of this, calcium peroxide (CaO_2) which can self-supply O_2 and H_2O_2 in contacting with water, has attracted much attention in the ROS-involved therapies [72]. As shown in Fig. 4c, manganese silicate (MSNs) loaded CaO_2 and indocyanine green (ICG) with further modified with lauric acid (LA,) has been synthesized to construct a H_2O_2/O_2 self-supplying thermoresponsive nanosystem, (MSNs@CaO_2-ICG)@LA [73]. LA as a phase-change material with melting point at 44-46 °C, can prevent the drug leakage and protect CaO_2 from water. After accumulated in tumor sites, the LA is melted by photothermal effect from ICG, and O_2 can be rapidly release from CaO_2 for further enhancing the PDT of ICG. Moreover, the self-supplied H_2O_2 from CaO_2 has also be verified to improve the EDT efficacy according to the recent work of our group [74]. As presented in Fig. 4d, a DCC-HA nanocomposite has been established using chloroperoxidase (CPO) and sodium-hyaluronate-modified CaO_2 co-loaded tetra-sulfide-bond-incorporating dendritic mesoporous organosilica (DMOS). Because of the immobilization of DMOS and the H_2O_2 supplement from CaO_2, CPO can generate more $^1O_2$ and induce OS in the mouse breast cancer cells.

The $^{\bullet}OH$ is another classical ROS of high activity, exhibiting harmful effects on DNA replication and cell membrane metabolism [75]. The generation of $^{\bullet}OH$ is mainly based on Fenton-type reaction, a catalytic reaction between H_2O_2 and several metal ions such as Fe^{2+} [76], Cu^{2+} [77], Mn^{2+} [78], Ti^{3+} [79] and Co^{2+} [80], which is defined as CDT in anti-tumor application. Glucose-oxidase (GOx) [81] and some noble metals [82] have been applied to catalyze the oxidation of glucose into H_2O_2 for CDT, but this process relies on oxygen that is lack in TME. Thus, metal peroxides self-supplying the H_2O_2 and metal ions for Fenton-type catalysis demonstrate certain superiority among other CDT agents. Chen's group first reported Fenton-type metal peroxide nanomaterials, copper peroxide (CP) nanodots, for the enhanced CDT by self-supplying H_2O_2 and Cu^{2+} (Fig. 5a) [83]. The CP nanodots with a hydrodynamic diameter of ~16.3 nm, were synthesized through coordination of H_2O_2 to Cu^{2+} with the assistance of OH^- and poly(vinylpyrrolidone) (PVP). Based on the enhanced permeability and retention (EPR) effect, the CP nanodots can accumulate at the tumor sites and exhibit a pH-dependent $^{\bullet}OH$ production property for cancer therapy. Very recently, our group reported a novel dual-metal (Ca^{2+} and Cu^{2+}) peroxides nanocomposite, CaO_2-CuO_2@HA NC, synthesized by the simultaneous coordination of H_2O_2 to Ca^{2+} and Cu^{2+} with the assistance of OH^- and hyaluronate (HA) (Fig. 5b) [84]. The HA endows the as-prepared NC chemical stability in aqueous solution and specific target function *in vivo*. In response to acid and hyaluronidase overexpressed TME, the CaO_2-CuO_2@HA NC not only provides sufficient H_2O_2 for Cu^{2+} based CDT, but also induces calcium overload, further leading to enhanced OS in tumor cells.

Among the above four therapeutic modes, PDT has the longest research history (about 100 years) and thus has the best theoretical and practical basis, whereas the light penetration depth greatly limits its application in deep-tissue lesions. The ultrasound exhibits more promising tissue penetration ability, while the mechanism of SDT is still not completely clear. The CDT is conducted based on the Fenton chemistry without any exogenous stimulus, while the relative high pH (6.0-7.0) of TME limits the dissolution of metal ions and efficiency of Fenton reaction. The chloroperoxidase (CPO) of EDT performs well in weak acidic TME, but the high cost of store and manufacture may be the primary issue before application. Therefore, developing ROS-regulating nanoplatform with multi-mode rather than mono-mode exhibits more potential for better antitumor efficacy.

3.1.2. Special gases

With the progress of nanotechnology and the development of interdisciplinarity, the strategy to improve ROS would not be confined to exogenous free radicals, some special gases also have a good performance. NO, CO, SO_2 and H_2 are special therapeutic gases for regulating many key biological functions in living organisms [85–87]. Emerging data reveal their redox regulation ability for anticancer after elevation their concentration beyond the certain threshold [88].

NO is a special gas, which is also known as the ROS or RNS. As a natural donor of NO, arginine (LA) also has been loaded to supply exogenous NO in tumor in response to H_2O_2 [89] or ultrasound (US) irradiation [90]. Inspired by these, our group fabricated a LA-loaded black mesoporous titania (BMT) (BMT@LA) NC, for US-triggered $^1O_2$ and NO generation at tumor sites (Fig. 6a) [91]. Interestingly, the US-excited $^1O_2$ can promote the NO generation from LA (Figs. 6b and c). The NO gas can lead to cellular OS, and the OS degree can be aggravated when cooperating with SDT, eventually leading to DNA double-strand breaks and the apoptosis of cancer cells (Fig. 6d). Similar to NO, CO has many physiological roles and also be applied in tumor inhibition using CO-releasing molecules (CORMs) [92–94]. However, the practical delivery and imprecisely controlled release of CO is risky due to the strong affinity toward Hb in the blood. To overcome these risks during practical usage, Wang *et al.* constructed a versatile *in situ* CO nanogenerator (designated as PPOSD) (Fig. 6e) [95]. The PPOSD was consist of partially oxidized tin disulfide (SnS_2) nanosheets (POS NSs), a tumor-targeting polymer (polyethylene glycol-cyclo(Asp-D-Phe-Lys-Arg-Gly), PEG-cRGD), and doxorubicin (DOX). Upon 561 nm laser irradiation, the PPOSD can photo-reduce the CO_2 to CO which further induce the mitochondrial collapse and cellular OS. Besides, the *in situ* generated CO can effectively sensitize cancer cells toward DOX for enhanced chemotherapy.

Like NO and CO, SO_2 is also a member of gasotransmitter family [86]. The SO_2 has a toxicological effect by inhalation with elevated concentrations, contributing to OS-induced damage of biomacromolecules [96]. In order to realize on-demand generation of SO_2 and minimize side effects, the Li *et al.* developed near-infrared (NIR) light-triggered SO_2 generation nanoplatform based on SO_2 prodrug (1-(2,5-dimethylthien-1,1-dioxide-3-yl)-2-(2,5-dimethylthien-3-yl)-hexafluorocyclopentene (DM) molecule) loaded upconversion@porous silica nanoparticles (abbreviated as RUCSNs-DM) (Fig. 7a) [97]. The efficient light conversion from 980 nm NIR light to UV light ensures the photolysis of DM to achieve on-demand release of SO_2 in deep tissues. The generated SO_2 is found to induce cell apoptosis by the increasing of intracellular ROS levels and causing damage of nuclear DNA. Except for the above therapeutic gas, H_2 also shows its significance in treating many diseases such as cancer [98], Alzheimer's disease [99], atherosclerosis [100], and diabetes [101] in past decades. The anticancer therapeutic mechanism of H_2 has been investigated by He's group using $PdH_{0.2}$ nanocrystals as the H_2 donor (Fig. 7b) [102]. The $PdH_{0.2}$ nanocrystals exhibit excellent photothermal ability and photothermal responsive H_2 release capability. After treated with H_2, the intracellular ROS level of cancer cells quickly declines due

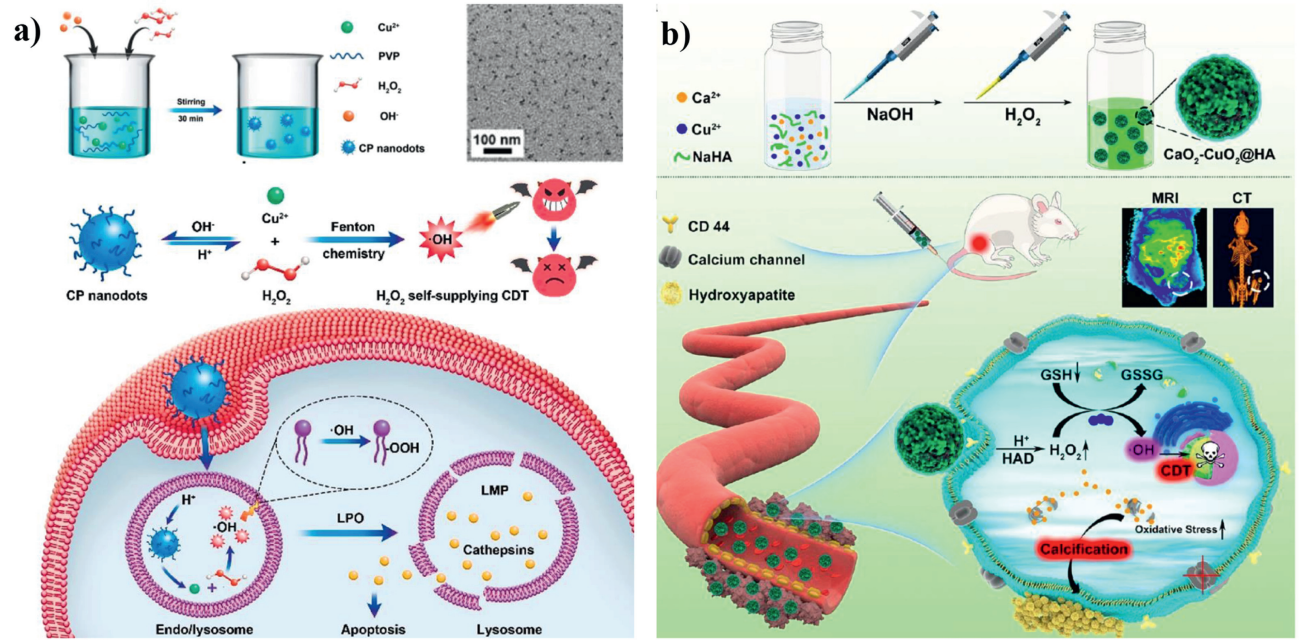

Fig. 5. (a) Schematic illustration of the synthesis and antitumor mechanism of PVP-coated CP nanodots. Reproduced with permission [83]. Copyright 2019, American Chemical Society. (b) Schematic illustration of the synthesis and antitumor performance of CaO_2-CuO_2@HA. Reproduced with permission [84]. Copyright 2022, American Chemical Society.

to the reduction effect of H_2, while it subsequently rebound because of the redox homoeostasis capability, and finally inducing strong OS in cancer cells (Fig. 7c). Compared with cancer cells, the normal cells are tolerable to this ROS regulation and show no obvious OS state (Fig. 7d). Gases have better diffusivity and could exhibit better therapeutic effect than free radicals *in vivo*. However, on the contrary, gas therapy relies more on precise targeting and controlled release to reduce more serious side effects.

3.2. Inhibiting the ROS elimination

It is worth noting that redox regulation in cancer cells is very complex, and simply adding ROS-generating agents would not lead to a preferential killing of cancer cells. Assist with elimination of high-level antioxidants cannot only improve the efficacy of oxidants, but also accelerate the redox imbalance toward OS.

3.2.1. Inhibiting redox-modulating enzymes

In the ROS elimination progress of cellular redox homoeostasis, SOD and CAT are the two important enzymes in cellular antioxidation system. Adding inhibitors of these enzymes helps achieve cellular OS. In view of this, Pan *et al.* reported a thioketal linked camptothecin (camptothecin prodrug, TK-CPT) and 2-methoxyestradiol (2-ME) loaded zeolitic imidazole framework-90 (ZIF-90) with finally coated with a layer of homologous cell membrane, 2-ME/TK-CPT@ZIF-90@C, for regulation of biochemical reactions in organelles and enhancement in the specificity of chemotherapeutic drugs (Fig. 8a) [103]. The 2-ME can inhibit the activity of SOD and induce the upregulation of ROS, thereby realiz-

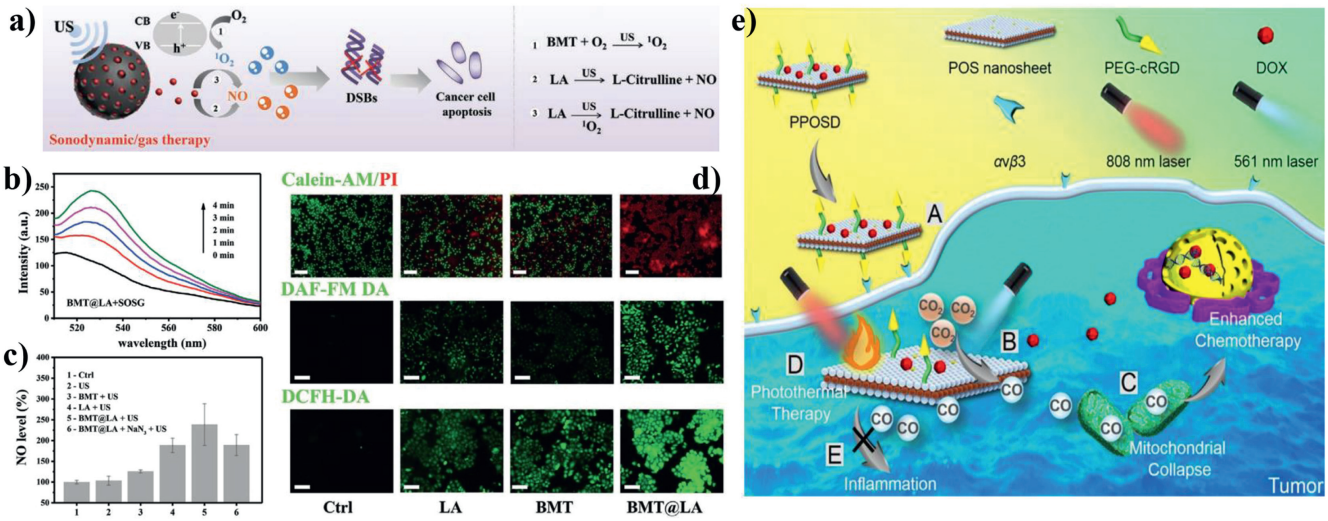

Fig. 6. (a) Schematic illustration of synergistic cancer sonodynamic/gas therapy mechanism of the BMT@LA. (b) US-triggered $^1O_2$ generation of BMT@L. (c) US-triggered NO generation ability of different group in HeLa cell. (d) Calcein-AM&PI dual staining, detection of NO generation, evaluation of the OS level. Reproduced with permission [91]. Copyright 2021, Wiley-VCH. (e) Schematic illustration of PPOSD for enhanced tumor inhibition. Reproduced with permission [95]. Copyright 2019, American Chemical Society.

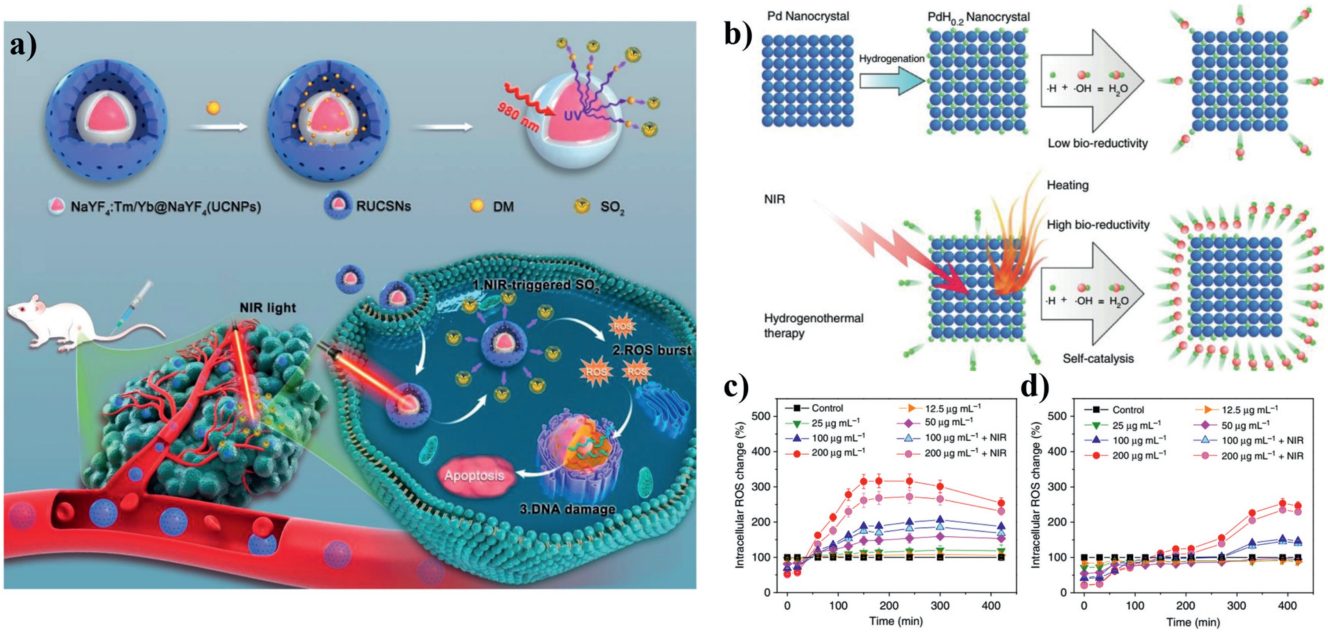

Fig. 7. (a) Schematic illustration of the synthesis and antitumor mechanism of RUCSNs-DM. Reproduced with permission [97]. Copyright 2019, American Chemical Society. (b) Schematic illustration of the synthesis and NIR-controlled H_2 release performance. The effect of $PdH_{0.2}$ nanocrystals on intracellular ROS levels in HeLa cells (c) and HEK-293T cells (d). Reproduced with permission [102]. Copyright 2020, Nature Publishing Group.

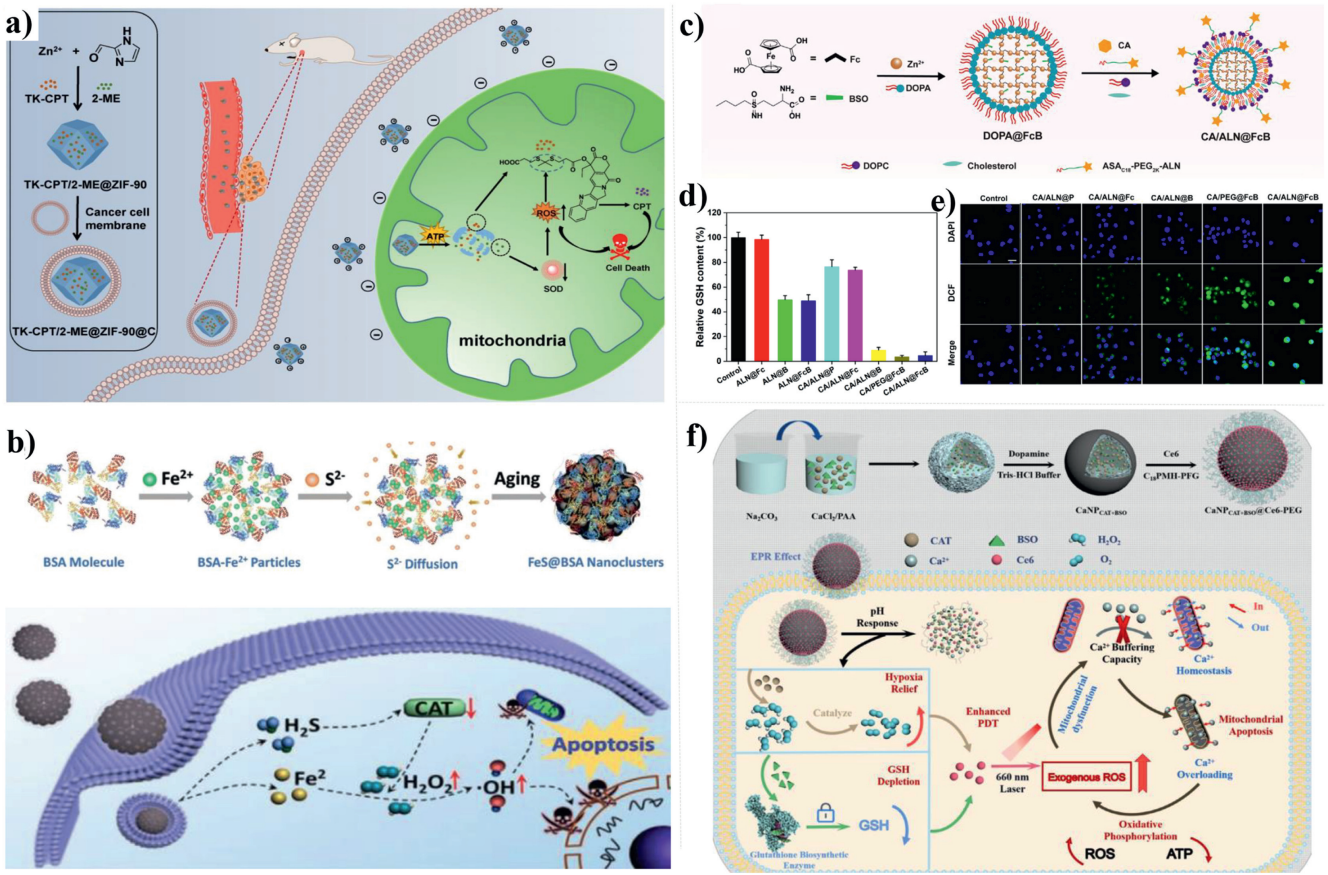

Fig. 8. (a) Schematic illustration of the synthesis and antitumor mechanism of 2-ME/TK-CPT@ZIF-90@C (MTZ@C). Reproduced with permission [103]. Copyright 2021, Ivyspring International Publisher. (b) Schematic illustration of the synthesis and synergistic therapeutic mechanism of FeS@BSA nanoclusters. Reproduced with permission [108]. Copyright 2020, Wiley-VCH. (c) Schematic illustration of the synthesis of CA/ALN@FcB. (d) GSH depletion performance of different groups. (e) ROS generation of different groups. Reproduced with permission [116]. Copyright 2020, Elsevier Ltd. (f) Schematic illustration of the synthesis and antitumor mechanism of of $CaNP_{CAT+BSO}$@Ce_6-PEG NPs. Reproduced with permission [117]. Copyright 2022, Elsevier Ltd.

ing subsequent release of parent CPT drug. The increased ROS level and liberation of CPT can lead to prolonged high OS and continuous apoptosis of cancer cells. Except for 2-ME, copper chelators (*e.g.*, ATN-224 [104]) and 3-amino-1,2,4-triazole (3-AT) [105] are verified as effective SOD and CAT inhibitors, respectively. Interestingly, CAT activity in some bacteria and plant cells has been proved to be regulated by H_2S in the recent explorations [106,107]. Inspired by that, Xie *et al.* fabricate the ferrous sulfide embedded bovine serum albumin (FeS@BSA) nanoclusters aiming to obtained enhanced CDT effect (Fig. 8b) [108]. The FeS@BSA nanoclusters can degrade and simultaneously release H_2S gas and Fe^{2+} ions in response to acidic condition. *In vitro* cellular experiments demonstrate that H_2S presents specific suppression effect to catalase activity and lead to the increasement of intracellular H_2O_2, significantly facilitating Fe^{2+}-based Fenton reaction and amplifying the ROS induction.

3.2.2. GSH depletion

Glutathione is an important endogenous antioxidant tripeptide, composed of glutamate (L-Glu), cysteine (L-Cys) and glycine (Gly). The -SH group on cysteine is the active group of reduced glutathione, thus the reduced glutathione is often abbreviated as GSH and the oxidized glutathione is abbreviated as GSSG. The reduced GSH plays a key role in the efficient operation of intracellular redox-regulating enzymes as the reducing equivalent [109]. In addition, GSH can also serve as ROS scavenger to reduce intracellular OS levels [110]. Therefore, overexpressed GSH (2-10 mmol/L) along with hypoxia and consumable H_2O_2 in TME are the three major obstacles of the development of ROS-mediated antitumor therapy [111].

The synthesis of GSH contains two ATP-dependent steps [112]. The first one is the linkage of L-Glu and L-Cys to form γ-Glu-Cys, which is catalyzed by the rate-limiting enzyme, glutamylcysteine synthetase (γ-GCS). The second one is linkage of Gly and γ-Glu-Cys to form GSH, catalyzed by glutamine synthetase. Many investigations have been reported to targeting the rate-limiting step for GSH depletion [113,114]. Buthionine sulphoximine (BSO) is found as an effective inhibitor of γ-GCS and widely used to enhance ROS level in cancer cells [115]. Huang *et al.* utilized the organic ligands of BSO and molecular Fenton catalyst 1,1′-ferrocenedicarboxylicacid (Fc) to coordinate with Zn^{2+} to fabricate the nanoscale coordination polymer (DOPA@FcB) [116]. And a hydrophobic shell was then constructed by coating 1,2-dioleoylsn-glycero-3-phosphocholine (DOPC) and cholesterol to load the small molecule drug cinnamaldehyde (CA) and alendronate (ALN)-functionalized amphipathic material, to form the final CA/ALN@FcB nanomaterials (Fig. 8c). As shown in Figs. 8d and e, the CA/ALN@FcB can deplete the cellular GSH level and enhanced the overall ROS level. Zhu *et al.* introduced a one-pot method to load the CAT and BSO, further modified with polydopamine (PDA) and photosensitizer chlorin e6 (Ce6) to obtain $CaNP_{CAT+BSO}$@Ce6-PEG NPs (Fig. 8f) [117]. CAT here was used for catalyzing the endogenous H_2O_2 to generate O_2. The PDT effect of Ce6 has been greatly improved after the relief of hypoxia and depletion of GSH.

Because GSH is highly reductive, the researchers have found that it can be oxidized into GSSG by many metal ions, thereby achieving GSH depletion. For example, the Fe^{3+} can oxidate GSH and itself turns into Fe^{2+} for Fenton reaction (Fig. 9a) [118]. After associated with cisplatin (CDDP), the lipid peroxidation (LPO) level of 4T1 cancer cells has been further upregulated (Figs. 9b and c). Recent years, our group has made many efforts on the GSH depletion assistive ROS regulation by various metal ions [119–121]. As shown in Fig. 9d, ICG loaded Cu-based MOFs has been synthesized for Cu^{2+} based GSH depletion and enhancing the Cu^{+}-mediated CDT. And the photothermal from NIR trigged ICG can further enhanced the CDT (Figs. 9e-g). Besides, the hollow structured Cu_2MoS_4 also exhibits excellent GSH depletion ability due to the existence of Cu^{+}/Cu^{2+} and Mo^{4+}/Mo^{6+} redox couple (Fig. 9h). After loading GOx, the CDT effect of the above redox couple can be further ensured (Figs. 9i and j). In addition, Mn^{2+} mediated GSH depletion has been presented in as-prepared MnO_x nanospikes (Fig. 9k). Interestingly, the Mn^{2+}-mediated CDT and GSH-depleting ferroptosis of MnO_x nanospikes can elicit immuogenic cell death and present a better synergistic immunopotentiation action along with antigen stimulations by MnO_x.

In addition to simply depletion for modulating redox homeostasis, the reducibility of GSH is also used to enhance ROS production processes. The tetravalent platinum Pt(IV) complexes (Pt(IV)) are a derivative of Pt(II) anticancer drug (Pt(II)) with different substitutions in the axial position, and can be reduced into toxic Pt(II) in cancer cells in the presence of GSH [122]. Xiang *et al.* constructed a TME responsive cascade nanoreactor (CuMOF@Pt(IV)) for the chemotherapy-enabled/augmented cascade catalytic tumor-oxidative nanotherapy (Fig. 10a) [123]. As shown in Figs. 10b and c, the GSH can be effectively consumed by both of CuMOF and Pt(IV). The decrease of GSH level and supplement of H_2O_2 through cisplatin-triggered cascade catalytic reactions can greatly enhance the ROS generation from Cu^{+}-mediated CDT (Figs. 10d and e). As we know, rapid recombination of photo-/sono-generated electron (e^{-}) and hole (h^{+}) is responsive for the poor PDT/SDT efficiency [124]. Creating an oxygen-deficient layer on the surface of semiconductor has been verified to improve charge-separation efficiency [125]. Recently, our group has reported a novel strategy of GSH-enhanced SDT, which utilized the endogenous GSH to convert Bi_2MoO_6 nanoribbons (BMO NRs) into GSH-activated Bi_2MoO_6 nanoribbons (GBMO NRs) (Fig. 11a) [126]. As shown in Figs. 11b-f, compared with BMO, the GBMO contains 17.43% of Mo^{5+} and a high content of oxygen vacancies, thus exhibiting much higher ability of ROS generation. Hence, the BMO can achieve two-step enhancement of SDT on cancer cells (Figs. 11g and h). Theoretically, h^{+} generated on the surface of catalyst has enough high oxidative capability ($\geq$0.32 eV) which is enough for GSH-to-GSSG evolution. Hence, He's group proposed the GSH can act as sacrificial agent and ensuring the long-term H_2 production from H^{+} reduced by e^{-} (Fig. 12a) [127]. The Z-scheme NIR-photocatalyst is synthesized consisting of highly oxidative (low valence band) plasmatic nanodots $SnS_{1.68}$ and NIR-activable (narrow band gap) semiconductor $WO_{2.41}$. As presented in Figs. 12b and c, the $SnS_{1.68}$-$WO_{2.41}$ nanocatalyst exhibits NIR-photocatalytic H_2 generation in the GSH (10 μmol/L) solution and NIR-photocatalytic GSH consumption behavior. The intracellular ROS level of $SnS_{1.68}$-$WO_{2.41}$-treated 4T1 cells persistently increased after the NIR irradiation, and maintains for a long term (>4.5 h) (Fig. 12d). Moreover, the GSH level of treated tumor sharply declines and the H_2 as well as ROS are largely generated, confirming the excellent results of synergistic antitumor therapy (Figs. 12e and f).

4. ROS-mediated tumor resistance alleviation

MDR and thermoresistance are the two common types of tumor resistance, and also the major reasons for the failure of chemotherapy and HTT, respectively. These resistances are mainly associated with redox status and expression/function of specific proteins in cancer cells. ROS has been widely investigated and applied in antitumor field with the rapid development of nanotechnology in recent decades, showing its powerful effects of downregulating specific proteins and killing cancer cells more effectively and safely. In the following sections, the cellular mechanism MDR and thermoresistance as well as recent examples of ROS regulation for alleviating tumor resistance will be illustrated respectively.

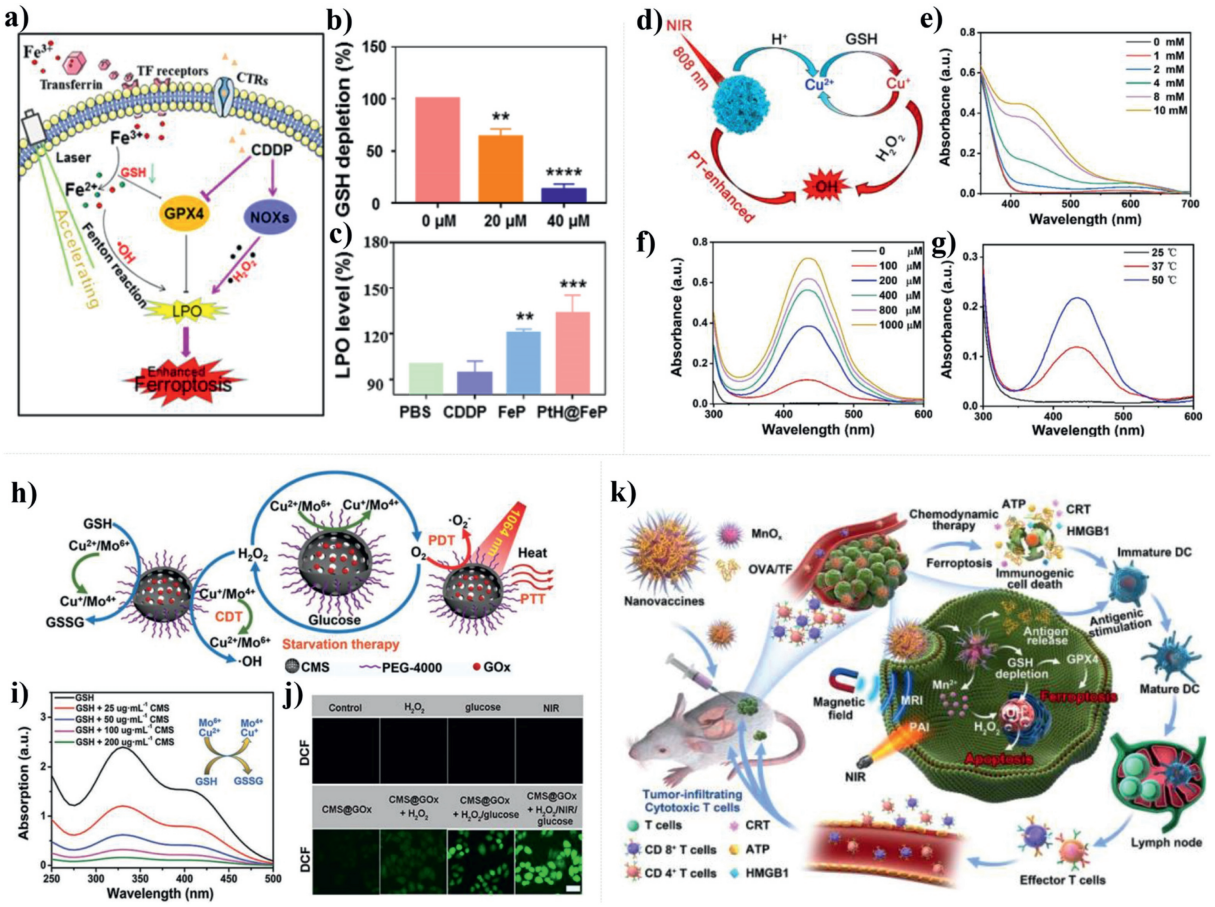

Fig. 9. (a) Schematic illustration of the synergistic antitumor effect of PtH@FeP. (b) GSH depletion of PtH@FeP in 4T1 cells. (c) LPO levels in 4T1 cells after treated with different formulations. Reproduced with permission [118]. Copyright 2021, American Chemical Society. (d) Schematic illustration of GSH depletion/photothermal-expanded ROS generation of ICG loaded Cu-based MOFs. GSH depletion (e), ·OH generation (f) and temperature enhanced ·OH generation (g). Reproduced with permission [119]. Copyright 2022, Elsevier Ltd. (h) Schematic illustration of fabrication and mechanism of PEGylated CMS@GOx for synergistic cancer therapy. GSH depletion (i) and ROS generation (j) ability of CMS@GOx. Reproduced with permission [120]. Copyright 2019, Wiley-VCH. (k) Schematic illustration of the synthesis and antitumor performance of the MnO_x-OVA/tumor cells fragment (TF) nanovaccines. Reproduced with permission [121]. Copyright 2020, Wiley-VCH.

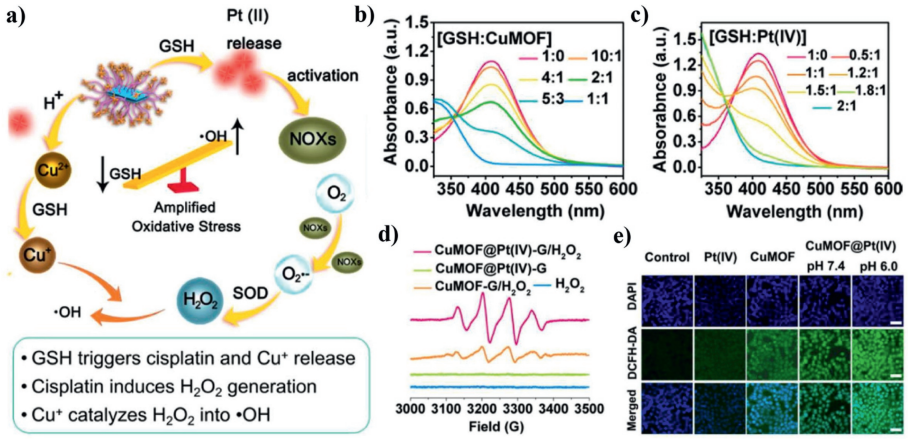

Fig. 10. (a) Schematic illustration of GSH depletion and ·OH generation of CuMOF@Pt(IV). (b, c) GSH depletion ability of CuMOF and Pt(IV). (d, e) ROS generation ability of CuMOF@Pt(IV). Reproduced with permission [123]. Copyright 2021, Elsevier Ltd.

4.1. MDR alleviation

4.1.1. Cellular mechanisms of MDR

The MDR of cancer cells can be conducted by several cellular factors, involving the increased efflux, decreased influx, activation of DNA repair, anti-apoptosis and so on [128–130]. Among these, drug efflux based on ATP-binding cassette (ABC) transporters is the most classical MDR mechanism [131]. The anthracyclines such as doxorubicin (DOX) are mainly affected by this mechanism [132]. Many preclinical studies and clinical trials have declared the benefit of inhibitors of ABC transporters such as MDR1/P-glycoprotein (P-gp) on mitigation of MDR [133–135]. Since the drug transport-

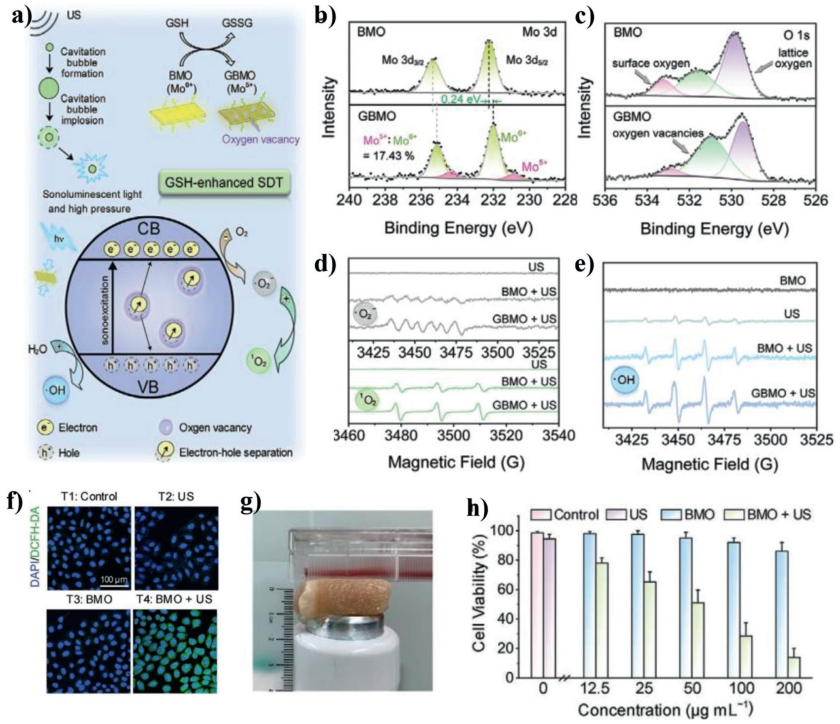

Fig. 11. (a) Proposed mechanism of BMO for GSH-enhanced SDT. (b, c) The content of Mo^{5+} and oxygen vacancies of BMO and GBMO. (d, e) US-triggered ROS generation ability of BMO and GBMO. (f) ROS level in HeLa cells. (g, h) *In vitro* simulated deep tissue sonodynamic effect of BMO. Reproduced with permission [126]. Copyright 2021, Wiley-VCH.

ing of P-gp is ATP-dependent, it is closely associated with the normal mitochondrial function and cellular redox state. Compared with DOX, the drug resistance of cisplatin is more closely related to the redox state of cancer cells. Firstly, the thiol-containing biomolecules, especially the GSH, can rapidly bind to internalized cisplatin to form a stable Pt-S bond adducts [136]. Then, these adducts will be transport out of cells by efflux protein ATP7A and ATP7B [137]. Since the ROS can affect proteins through its synthesis, function and stability, regulating the redox state in cancer cells seems to be a potential approach for MDR alleviation.

4.1.2. ROS regulation for MDR alleviation

As ATP is essential for the transporting function of P-gp, the MDR could be overcome by decreasing the ATP level in cancer cells. The He's group constructed a lipid membrane-coated silicacarbon (LSC) hybrid nanoparticle that can specifically produce ROS in mitochondria under NIR irradiation [138]. As shown in Figs. 13a-d, the NIR triggered ROS can decrease the nicotinamide adenine dinucleotide with hydrogen (NADH) by oxidizing it into NAD^+, which decreases the concentration gradient of protons in mitochondria and reduces the production of ATP. Thus, the expression

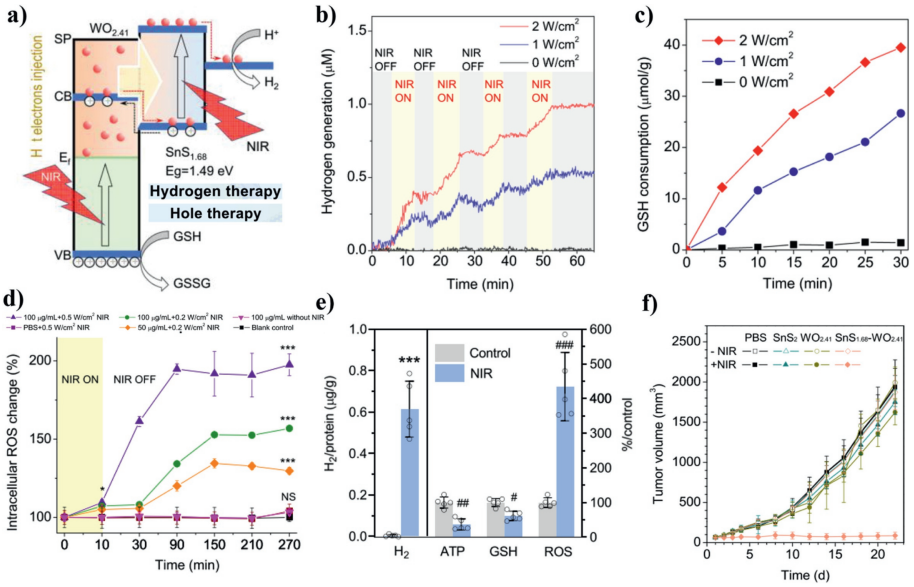

Fig. 12. (a) Schematic illustration of NIR photocatalytic H_2 generation and GSH consumption of $SnS_{1.68}$-$WO_{2.41}$. (b) NIR-photocatalytic hydrogen generation behavior in the GSH (10 μmol/L) aqueous solution and (c) the GSH consumption behavior of $SnS_{1.68}$-$WO_{2.41}$. (d) Intracellular ROS change before and after NIR irradiation. (e) Intratumoral H_2, ATP, GSH, and ROS levels before and after NIR irradiation. (f) Antitumor effect of $SnS_{1.68}$-$WO_{2.41}$. Reproduced with permission [127]. Copyright 2021, Nature Publishing Group.

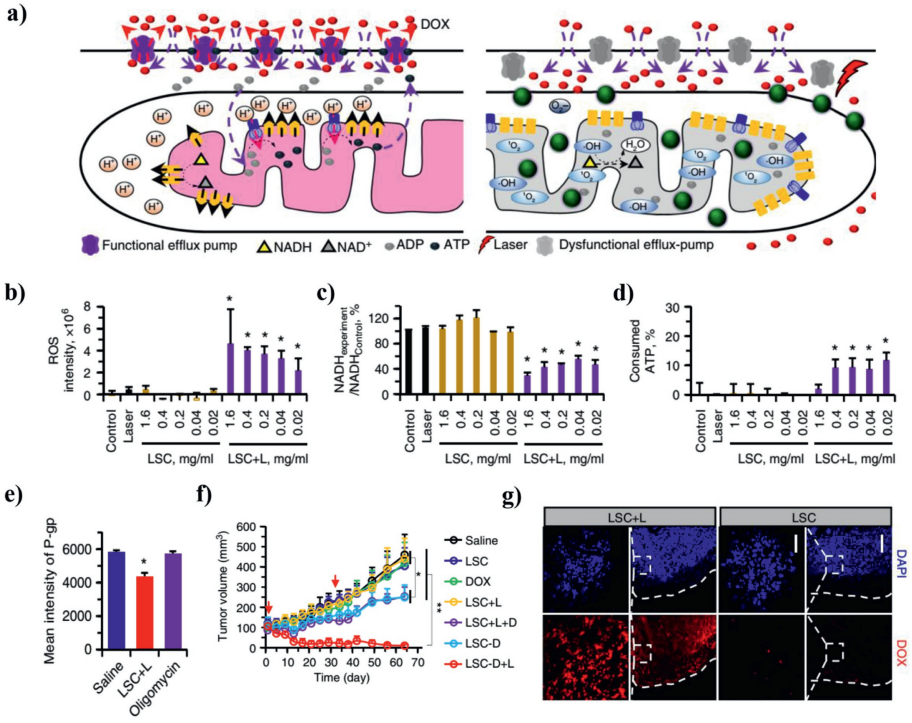

Fig. 13. (a) Schematic illustration of the mechanism of overcoming MDR by the LSC Nanoparticles. (b-d) The ROS, relative NADH, consumption of ATP in LSC treated NCI/RES-ADR cells before and after NIR irradiation. (e) The expression of P-gp protein. (f) Synergistic antitumor effect. (g) Drug-resistant recovery of the NCI/RES-ADR cells in the tumors with the LSC-D + L treatment. Reproduced with permission [138]. Copyright 2018, Nature Publishing Group.

of P-gp is significantly decreased in the RES-ADR (doxorubicin-resistant) cancer cells with the LSC + L treatment (Fig. 13e). The excellent inhibition effect can be observed in the DOX-laden LSC (LSC-D) + L group (Fig. 13f). After being treated for 64 days, the tumor cells were then collected and incubated with DOX to investigate the reversal of MDR. The fluorescence images of DOX show that the uptake of DOX has been greatly improved (Fig. 13g). The SO_2 is a potential gas for efficient cellular OS regulation in the previous investigations. Wang *et al.* [139] synthesized MON-DN@PCBMA-DOX, consist of SO_2 prodrug molecules (DN, 2,4-dinitrobenzenesulfonylchloride) and DOX loaded and zwitterionic polymer coated mesoporous organosilica nanoparticle to construct the GSH-responsive SO_2/DOX released nanosystem (Fig. 14a). The high level of cellular SO_2 and ROS can be observed in the Flow cytometry analysis in Figs. 14b and c, thus reducing the expression of P-gp protein and enhancing the uptake amount of DOX in doxorubicin-resistant MCF-7 (MCF-7/ADR cells) (Figs. 14d-f).

GSH have been verified to promote the detoxification of cisplatin under the catalysis of glutathione S-transferases (GST) in the cisplatin-resistant cancer cells [140]. Niu and co-works synthesized S-S-bridged hollow mesoporous organosilica hybrid nanoparticles (SHMONs) for the loading of cisplatin (CisPt) and GST inhibitor (ethacrynic acid, EA) to form (CisPt+EA)@SHMONs (Fig. 15a) [141]. The cellular GSH level can be obviously depleted due to the existent of S-S bond in SHMONs, thus inducing OS in CisPt-resistant A375/DDP cells (Figs. 15b and c). Compared with other group, the Pt content of whole the cell and genomic DNA in (CisPt+EA)@SHMONs treated A375/DDP group has been increased significantly, revealing the alleviation of drug resistance (Figs. 15d-f). Except for preventing detoxification, decreasing efflux of cisplatin is also critical. Ge *et al.* developed a smart network based on MoS_2/CF_3SO_2Na nanoparticles (HA@$MoCF_3$ NPs) with sonodynamic and nanoenzymatic properties (Fig. 16a) [142]. Large amount of $^{\bullet}O_2^-$, $^{\bullet}OH$, $^{\bullet}CF_3$ and SO_2 can be generated from HA@$MoCF_3$ NPs *via* cascade reactions under US irradiation, causing the damage of ATP7B efflux protein and failure of DNA repair (Figs. 16b and c). The ATP production has been inhibited due to the ROS-mediated mitochondria dysfunction, further inhibit the function of ATP7B (Figs. 16d-f). Thus, a series of ROS mediated regulation containing reducing efflux, preventing detoxification, inhibiting DNA repair have been conducted in this work for a comprehensive reversal of cisplatin resistance.

4.2. Thermoresistance alleviation

4.2.1. Cellular mechanisms of thermoresistance

In the past decades, HTT that causes local high temperature of tumor sites for tumor ablation shows its effectiveness in preclinical studies and some clinical trials [143–145]. The exogenous stimulation, such as NIR light, magnetic field, US, and radiofrequency, are essential for a HTT process [146]. It has been proved that overexpressed HSPs (especially HSP70 and HSP90) are the major reason of tumor thermoresistance [147]. The HSPs are a type of stress-inducible proteins, which can be rapidly produced under elevated heat to repair the fever-type cell damages and inhibit caspase-independent apoptosis [148]. Low-temperature HTT (less than 45 °C) avoids the intense adverse effects on human bodies, thus receiving increasing attention [149]. However, compared with high-temperature thermal ablation (>50 °C), the effects of low-temperature HTT can be much more compromised due to the overexpression of HSPs. Therefore, downregulating HSPs is imperative to the alleviation of thermoresistance and the development of HTT, especially the low-temperature HTT.

4.2.2. ROS regulation for thermoresistance alleviation

It has been found that the expression of HSP70 and HSP90 with high molecular weights are curiously dependent on cellular ATP level [150]. Therefore, the excess ROS with high activity has the potential to paly similar roles on the

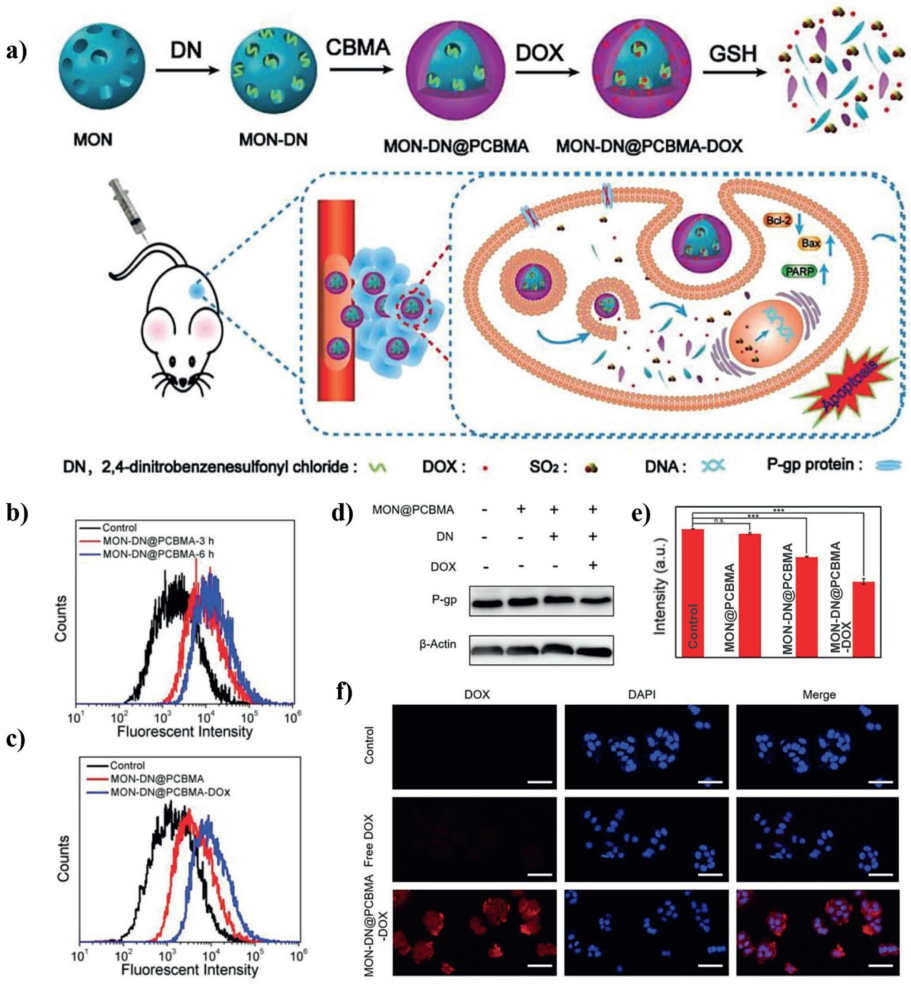

Fig. 14. (a) Schematic illustration of redox-responsive sulfur dioxide–releasing nanosystem and combination therapy. (b, c) The production of SO_2 and ROS in MCF-7/ADR cells. (d, e) The expression of P-gp protein. (f) DOX uptake ability of MCF-7/ADR cells after different treatments. Reproduced with permission [139]. Copyright 2020, Wiley-VCH.

thermoresistance alleviation as it on MDR. Ying *et al.* constructed the GOx-loaded hollow iron oxide nanocatalysts (HIONCs) for starvation/chemodynamic/magnetic-thermal synergistic cancer therapy (Fig. 17a) [151]. The mild temperature increasing of around 43 °C at tumor sites can be realized after exposure to the magnetic field (Figs. 17b and c). More interestingly, the mild increasing of temperature and acidic condition can improve the chemodynamic generation of highly toxic ·OH (Fig. 17d). The ROS generation and glucose consumption can suppress the expression of HSP70 and HSP90, which further enhances the magnetic-thermal therapy (Fig. 17e). In addition to downregulation of HSPs, the ROS such as LPO has provided a novel tactics to cleave HSPs [152]. Thus, our group constructed a NIR-II responsive Pd SAzyme for ferroptosis-boosted mild PTT (Fig. 17f) [153]. The Pd SAzyme exhibits excellent 1064 nm light triggered photothermal ability and the photothermal conversion efficiency (η) is calculated to be 33.98%. The Pd SAzyme with atom-economic utilization of the catalytic centers exhibits peroxidase (POD)-like activity to produce ·OH and glutathione oxidase (GSHOx) mimic activity to deplete GSH in the mimic environment of acid (pH 6.5) and mild therapeutic temperature (42 °C) (Figs. 17g and h). The obvious accumulation of LPO can be detected in Pd SAzyme treated 4T1 cells after 1064 nm laser irradiation, which further induces the HSPs damage and enhances mild-temperature PTT (Figs. 17i-k). In addition, CO has been found to target cellular mitochondria and inhibit its respiration, thus modulating cellular ATP levels in cancer cells [154]. Yao *et al.* reported an NIR-II light-controlled CO nanogenerator (Pd@PdCO-MOF) based on Pd nanosheet core and a porphyrin-Pd metal-organic framework (Pd-MOF) shell which coordinates large amounts of CO with Pd atom (Fig. 18a). The excellent NIR-II light triggered photothermal effect of Pd@PdCO-MOF can further promote the release of CO (Fig. 18b) [155]. Significant enhancement of tumor inhibition can be observed in the CO/PTT synergistic cancer therapy (Fig. 18c). The mechanism for the CO-mediated enhancement in PTT has been confirmed to be the downregulation of HSP70 expression after the mitochondrial dysfunction (Figs. 18d and e).

5. Summary and perspectives

The cancer cells endow evolved redox adaption to the high level of endogenous ROS to maintain their proliferation and metastasis activities, which inversely makes them sensitive to external interference with their redox state. In the past decades, great efforts have been made on manipulating this redox balance for enhanced tumor suppression. Two feasible strategies, including increasing the ROS generation and inhibiting the ROS elimination have been applied to the ROS-mediated cancer therapy. Numerous novel therapeutic modes have been developed based on the classical radicals and special therapeutic gases, revealing their redox regulation ability for inducing cellular OS. On other hand, several chemical agents have been verified to behave well in decreasing or inhibiting the

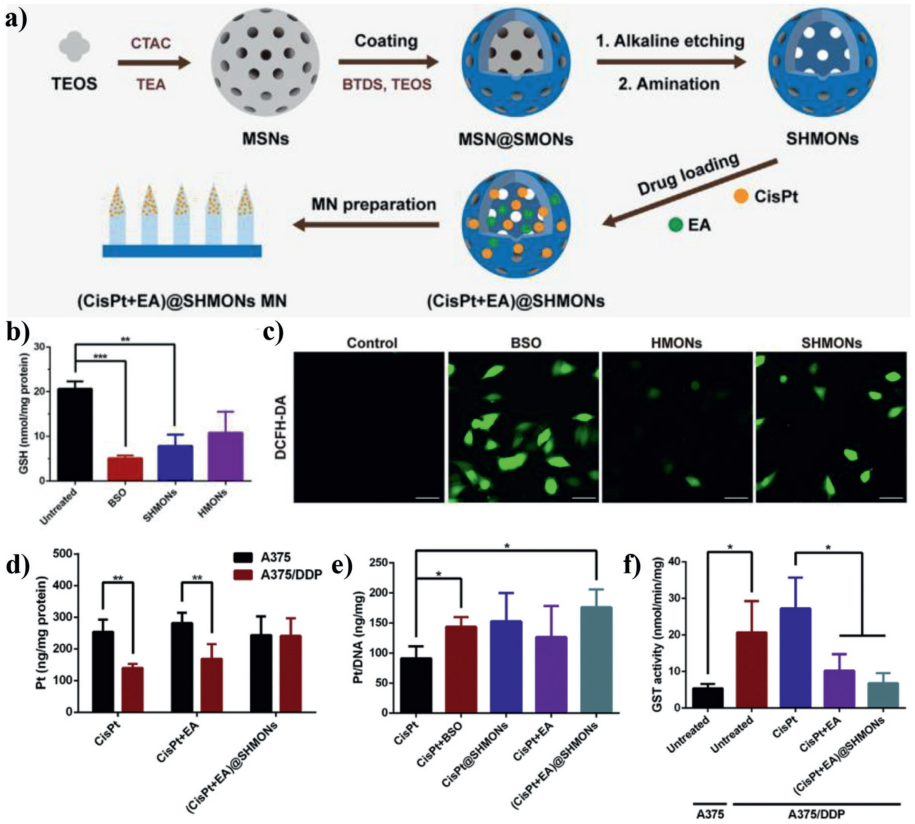

Fig. 15. (a) Schematic illustration of the fabrication of nanomedicine (CisPt+EA)@SHMONs. (b, c) The GSH depletion and ROS generation of A375/DDP cells after different treatments. (d) Pt uptake of A375 cells and A375/DDP cells. (e) Pt content in the genomic DNA of A375/DDP cells. (f) GST activity of A375 cells and A375/DDP cells. Reproduced with permission [141]. Copyright 2022, Elsevier Ltd.

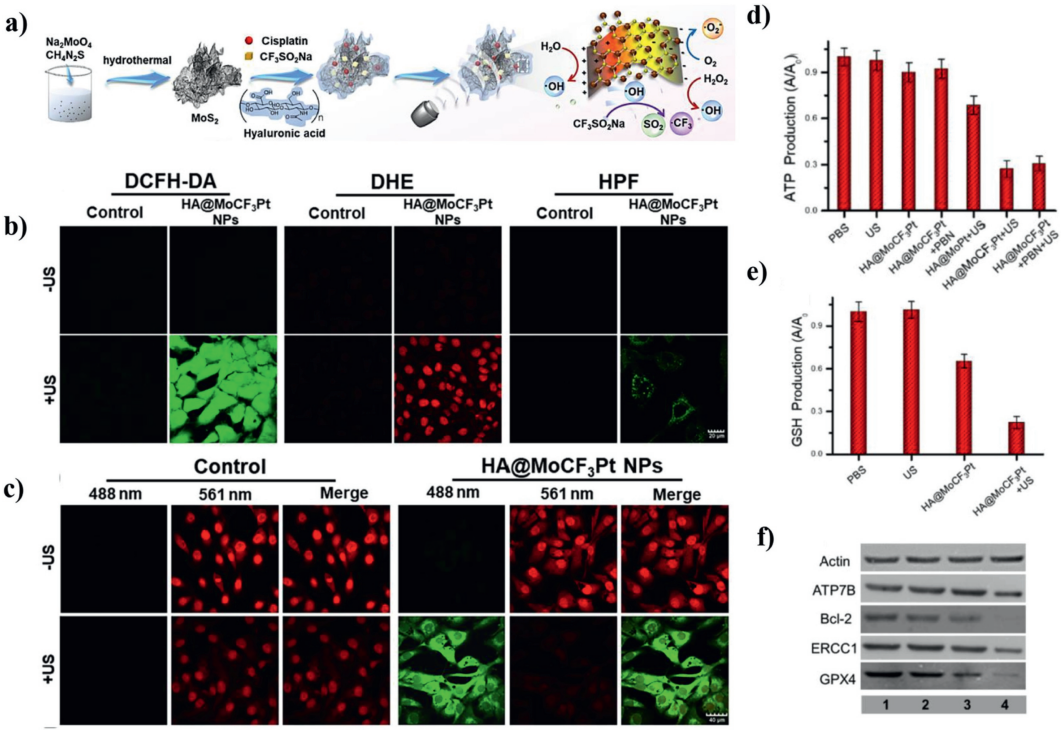

Fig. 16. (a) Schematic illustration of ·OH, ·CF_3 and SO_2 formation process of HA@$MoCF_3Pt$ NPs. (b) ROS, ·O_2^- and ·OH generation in SKOV-3/DDP cells. (c) Production of SO_2 in SKOV-3/DDP cells. (d, e) Content of ATP and GSH in SKOV-3/DDP cells after different treatments. (f) Expression of ATP7B protein in SKOV-3/DDP cells after different treatments. Reproduced with permission [142]. Copyright 2022, Elsevier Ltd.

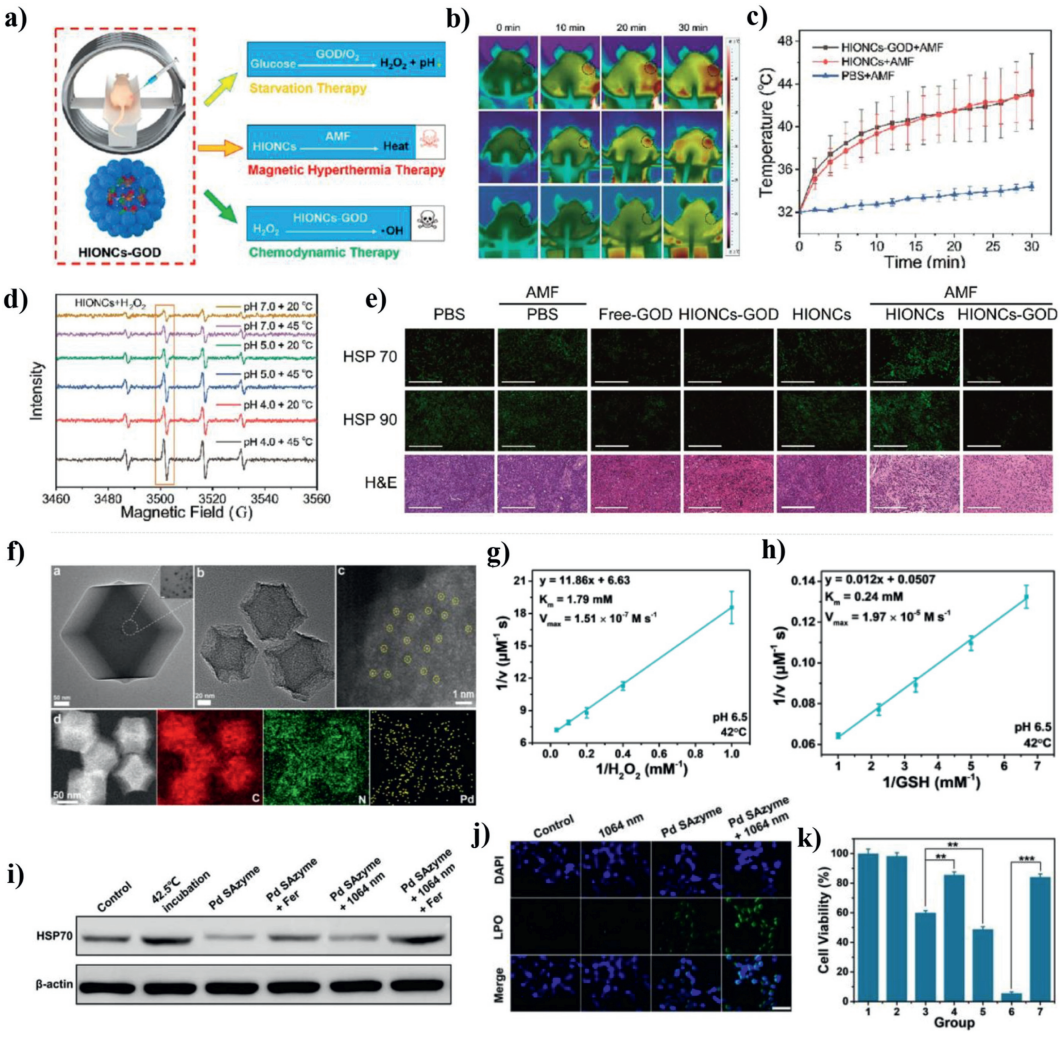

Fig. 17. (a) Schematic illustration of synergistic antitumor effect of HIONCs-GOD. (b, c) Temperature changes of tumor sites after exposure to the magnetic field. (d) ROS generation at different temperature and pH condition. (e) Expression of HSP70 and HSP90 in tumor. Reproduced with permission [151]. Copyright 2020, American Chemical Society. (f) TEM image of Pd@ZIF-8. (g, h) The POD and GSHOx-mimic enzyme activities of Pd SAzyme. (i, j) Expression of HSP70 and LPO level in 4T1 cells after different treatments. (k) Cytotoxicity assessment on 4T1 cells with different treatments. Reproduced with permission [153]. Copyright 2021, Wiley-VCH.

anti-oxidants. Moreover, the anti-oxidant such as GSH, can also act as reductant or sacrificial agent in the chemical reactions for enhancing ROS production. In addition, numerous works have shown that ROS regulation in cancer cells can inhibit the expression and function of resistance-related proteins such as MDR-related efflux proteins and thermoresistance-related HSPs, thus showing excellent performances in tumor resistance alleviation and enhanced synergistic cancer therapy. However, there still exists some considerable challenge of the ROS regulation in this stage before the practical clinic antitumor applications:

(1) Strict control of ROS level *in vivo*. In recent years, researchers usually only focus on the design of nanomaterials to enhance therapeutic efficacy and reduce side effects [156,157]. However, ROS present dual effects on cancer cells *in vivo*. The moderate increase of ROS level would promote the aggressiveness of tumor and poor prognosis [158], and the sharp increase of ROS level could be harmful to ambient normal tissues [159]. Thus, it is urgent to develop the *in vivo* real-time quantitative measurement of redox status to optimize the practical ROS dose and guide the ROS-mediated precision medicine.

(2) Reaction mechanisms in intracellular environment. Numerous novel therapeutic modes have been developed based on the light or US triggered catalytic reactions, even involving cellular cascade catalytic reactions. However, unlike *in vitro* solutions that only contain reactants we needed, the intracellular compositions are very complex with all in one, and the actual chemical reactions might be much different than those we excepted. Thus, more investigations on the reaction mechanism in actual intracellular environment are needed to improve the efficiency and precision of ROS regulation.

(3) The safety of ROS regulating nanoagents. The safety is the most critical issues. To date, most of the nanoagents used for ROS regulation are constructed based on inorganic nanomaterials because of their excellent chemical stability and easy functionalization. Although the inorganic nanomaterials perform well in preclinical examinations of small animals such as mice and rabbits. in some degree, most approved drugs are limited type of chemo drugs based organic nanosystems with well degradability [160]. Although more and more researches are focused on improving responsive biodegradation of nanoagents to reduce their accumulation in the normal organs [161], the risk of the metal ions released after degradation is still unknown. Therefore, more systematic studies are necessary to be conducted on the long-term effects of inorganic nanomaterials on animals or humans.

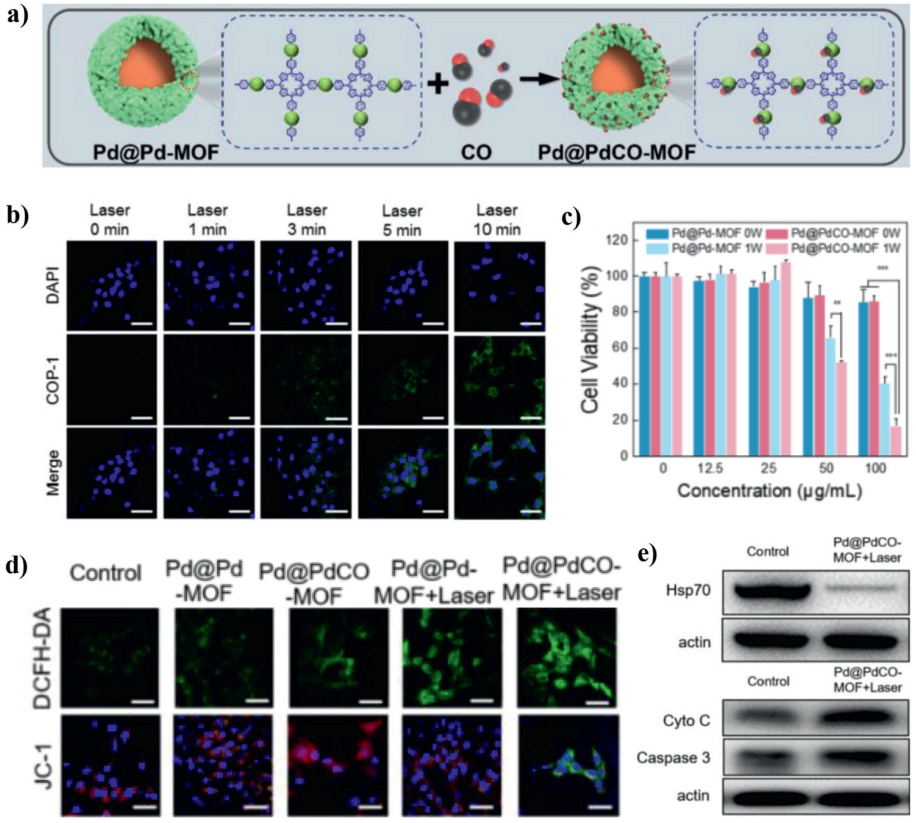

Fig. 18. (a) Schematic illustration of construction of Pd@PdCO-MOF. (b) NIR-II-controlled CO release in 4T1 cells. (c) Viability of 4T1 cells. (d) ROS generation and mitochondrial membrane hyperpolarization in 4T1 cells. (e) Expression of HSP70 in 4T1 cells. Reproduced with permission [145]. Copyright 2022, Elsevier Ltd.

Finally, great progresses have been made in cellular ROS regulation and ROS-mediated tumor resistance alleviation based on nanoplatforms, which has significantly promoted the development of ROS-based therapy, chemotherapy, hyperthermia therapy, as well as synergistic oncotherapy. With the in-depth investigation of the mechanisms and development of the nanotechnology, precision medicine based on ROS regulation will bring more benefits to cancer patients.

Declaration of competing interest

The authors declare that they have no known competing financial interests or personal relationships that could have appeared to influence the work reported in this paper.

Acknowledgments

This work is financially supported by the National Key Research and Development Program of China (No. 2022YFB3804500), the National Natural Science Foundation of China (NSFC, Nos. 51929201 and 52102354), and the projects for Science and Technology Development Plan of Jilin province (Nos. 20210402046GH and 20220508089RC).

References

[1] J.D. Hayes, A.T. Dinkova-Kostova, K.D. Tew, Cancer Cell 38 (2020) 167–197.
[2] J.E. Klaunig, Curr. Pharm. Des. 24 (2018) 4771–4778.
[3] S. Rezatabar, A. Karimian, V. Rameshknia, et al., J. Cell. Physiol. 234 (2019) 14951–14965.
[4] B. Perillo, M. Di Donato, A. Pezone, et al., Exp. Mol. Med. 52 (2020) 192–203.
[5] U.S. Srinivas, B.W. Tan, B.A. Vellayappan, et al., Redox. Biol. 25 (2019) 101084.
[6] D. Jia, X. Ma, Y. Lu, et al., Chin. Chem. Lett. 32 (2021) 162–167.
[7] J. Zhang, D. Duan, Z.L. Song, et al., Med. Res. Rev. 41 (2021) 342–394.
[8] Q. Wang, Z. Gao, K. Zhao, et al., Chin. Chem. Lett. 33 (2022) 1917–1922.
[9] C. Xu, R. Song, P. Lu, et al., Int. J. Nanomed. 15 (2020) 65.
[10] S. Yang, K.H. Wong, P. Hua, et al., Acta Biomater. 140 (2022) 492–505.
[11] D. Wu, Y. Fan, H. Yan, et al., Chem. Eng. J. 404 (2021) 126481.
[12] G. Lu, X. Gao, H. Zhang, et al., Chin. Chem. Lett. 33 (2022) 1923–1926.
[13] M. Yang, T. Yang, C. Mao, Angew. Chem. Int. Ed. 58 (2019) 14066–14080.
[14] X. Wang, X. Zhong, F. Gong, et al., Mater. Horiz. 7 (2020) 2028–2046.
[15] X. Wang, X. Wang, Q. Yue, et al., Nano Today 39 (2021) 101170.
[16] J. Zhu, A. Ouyang, Z. Shen, et al., Chin. Chem. Lett. 33 (2022) 1907–1912.
[17] S.L. Li, P. Jiang, F.L. Jiang, et al., Adv. Funct. Mater. 31 (2021) 2100243.
[18] X. Zhang, C. He, Y. Chen, et al., Biomaterials 275 (2021) 120987.
[19] S. Wang, H. Liao, F. Li, et al., Chin. Chem. Lett. 30 (2019) 847–852.
[20] X. Chang, Q. Wu, Y. Wu, et al., Nano Lett. 22 (2022) 8321–8330.
[21] X. Wang, Q. Wang, Acc. Chem. Res. 54 (2021) 1274–1287.
[22] Q. Wu, Z. He, X. Wang, et al., Nat. Commun. 10 (2019) 240.
[23] M. Wan, Z. Liu, T. Li, et al., Angew. Chem. Int. Ed. 60 (2021) 16139–16148.
[24] Y. Wu, M. Yuan, J. Song, et al., ACS Nano 13 (2019) 8505–8511.
[25] Y. Wang, T. Yang, Q. He, Natl. Sci. Rev. 7 (2020) 1485–1512.
[26] L. Kou, R. Sun, S. Xiao, et al., ACS Appl. Mater. Interfaces 11 (2019) 26722–26730.
[27] Y. Oh, H.R. Jung, S. Min, et al., Cancer Lett. 497 (2021) 123–136.
[28] M. Faustova, E. Nikolskaya, M. Sokol, et al., Free Radic. Biol. Med. 143 (2019) 522–533.
[29] B. Heym, N. Honoré, C. Schurra, et al., Lancet 344 (1994) 293–298.
[30] A. Persidis, Nat. Biotechnol. 17 (1999) 94–95.
[31] Y. Qiao, Z. Wei, T. Qin, et al., Chin. Chem. Lett. 32 (2021) 2877–2881.
[32] P.R. Stauffer, Int. J. Hyperth. 21 (2005) 731–744.
[33] D.K. Chatterjee, P. Diagaradjane, S. Krishnan, Ther. Deliv. 2 (2011) 1001–1014.
[34] K. Li, M. Lu, X. Xia, et al., Chin. Chem. Lett. 32 (2021) 1010–1016.
[35] M.H. Manjili, X.Y. Wang, J. Park, et al., Int. J. Hyperth. 18 (2002) 506–520.
[36] F.C. Lin, C.H. Hsu, Y.Y. Lin, Int. J. Nanomed. 13 (2018) 3529.
[37] J. Landry, D. Bernier, P. Chrétien, et al., Cancer Res. 42 (1982) 2457–2461.
[38] Y. Tabuchi, I. Takasaki, S. Wada, et al., Int. J. Hyperth. 24 (2008) 613–622.
[39] T. Finkel, IUBMB Life 52 (2001) 3–6.
[40] O. Augusto, S. Miyamoto, Oxygen radicals and related species, in: K. Pantopoulos, H.M. Schipper (Eds.), Principles of Free Radical Biomedicine, Nova Science Publishers Inc., New York, 2011, pp. 19–42.
[41] M. Inoue, E.F. Sato, M. Nishikawa, et al., Curr. Med. Chem. 10 (2003) 2495–2505.
[42] S. Wang, B. Zhu, B. Wang, et al., Chin. Chem. Lett. 32 (2021) 1795–1798.
[43] H. Sumimoto, FEBS J. 275 (2008) 3249–3277.
[44] W. Lu, M.A. Ogasawara, P. Huang, Drug Discov. Today 4 (2007) 67–73.
[45] D.B. Zorov, M. Juhaszova, S.J. Sollott, Physiol. Rev. 94 (2014) 909–950.

[46] Y. Ding, J. Wan, Z. Zhang, et al., ACS Appl. Mater. Interfaces 10 (2018) 4439–4449.
[47] P. Ferdinandy, R. Schulz, Br. J. Pharmacol. 138 (2003) 532–543.
[48] J. Zhang, Y. Fu, P. Yang, et al., Adv. Mater. Interfaces 7 (2020) 2000632.
[49] A.S. Kamiguti, L. Serrander, K. Lin, et al., J. Immunol. 175 (2005) 8424–8430.
[50] G. Martinez-Sanchez, A. Giuliani, J. Exp. Clin. Cancer Res. 26 (2007) 39.
[51] B. Kumar, S. Koul, L. Khandrika, et al., Cancer Res. 68 (2008) 1777–1785.
[52] Y. Hu, D.G. Rosen, Y. Zhou, et al., J. Biol. Chem. 280 (2005) 39485–39492.
[53] L. Behrend, G. Henderson, R.M. Zwacka, Biochem. Soc. Trans. 31 (2003) 1441–1444.
[54] D. Komatsu, M. Kato, J. Nakayama, et al., Oncogene 27 (2008) 4724–4732.
[55] W.S. Wu, Cancer Metast. Rev. 25 (2006) 695–705.
[56] D. Trachootham, J. Alexandre, P. Huang, Nat. Rev. Drug Discov. 8 (2009) 579–591.
[57] J. Kim, J. Kim, J.S. Bae, Exp. Mol. Med. 48 (2016) e269.
[58] Z. Zhou, J. Song, R. Tian, et al., Angew. Chem. Int. Ed. 129 (2017) 6592–6596.
[59] S. Son, J.H. Kim, X. Wang, et al., Chem. Soc. Rev. 49 (2020) 3244–3261.
[60] Y. Qin, L.J. Chen, F. Dong, et al., J. Am. Chem. Soc. 141 (2019) 8943–8950.
[61] L. Zhang, D. Wang, K. Yang, et al., Adv. Sci. 5 (2018) 1800049.
[62] Y. Wang, J. Yu, Z. Luo, et al., Adv. Mater. 33 (2021) 2103497.
[63] Y. Liu, X. Zhao, C. Zhao, et al., Small 15 (2019) 1901254.
[64] M. Yuan, S. Liang, Y. Zhou, et al., Nano Lett. 21 (2021) 6042–6050.
[65] Q. Chen, J. Chen, Z. Yang, et al., Adv. Mater. 31 (2019) 1802228.
[66] W. Zhu, Z. Dong, T. Fu, et al., Adv. Funct. Mater. 26 (2016) 5490–5498.
[67] S. Liang, X. Deng, G. Xu, et al., Adv. Funct. Mater. 30 (2020) 1908598.
[68] Y. Zhu, W. Wang, J. Cheng, et al., Angew. Chem. Int. Ed. 60 (2021) 9480–9488.
[69] J. Li, M.F. Stephanopoulos, Y. Xia, Chem. Rev. 120 (2020) 11699–11702.
[70] D. Wang, H. Wu, S.Z.F. Phua, et al., Nat. Commun. 11 (2020) 357.
[71] L. Zhang, S.S. Wan, C.X. Li, et al., Nano Lett. 18 (2018) 7609–7618.
[72] M. Zhang, R. Song, Y. Liu, et al., Chem 5 (2019) 2171–2182.
[73] C. Liu, Y. Cao, Y. Cheng, et al., Nat. Commun. 11 (2020) 1735.
[74] B. Liu, S. Liang, Z. Wang, et al., Adv. Mater. 33 (2021) 2101223.
[75] L. Zhang, X. Wang, R. Cueto, et al., Redox. Biol. 26 (2019) 101284.
[76] C. Xue, M. Li, C. Liu, et al., Angew. Chem. Int. Ed. 60 (2021) 8938–8947.
[77] L. Chudal, N.K. Pandey, J. Phan, et al., ACS Appl. Bio Mater. 3 (2020) 1804–1814.
[78] B. Ding, S. Shao, F. Jiang, et al., Chem. Mater. 31 (2019) 2651–2660.
[79] X. Wang, X. Zhong, L. Bai, et al., J. Am. Chem. Soc. 142 (2020) 6527–6537.
[80] J. Dong, L. Song, J.J. Yin, et al., ACS Appl. Mater. Interfaces 6 (2014) 1959–1970.
[81] C. Fang, Z. Deng, G. Cao, et al., Adv. Funct. Mater. 30 (2020) 1910085.
[82] S. Gao, H. Lin, H. Zhang, et al., Adv. Sci. 6 (2019) 1801733.
[83] L.S. Lin, T. Huang, J. Song, et al., J. Am. Chem. Soc. 141 (2019) 9937–9945.
[84] B. Liu, Y. Bian, S. Liang, ACS Nano 16 (2021) 617–630.
[85] C. Szabo, Nat. Rev. Drug Discov. 15 (2016) 185–203.
[86] Y. Huang, C. Tang, J. Du, et al., Oxid. Med. Cell. Longev. 2016 (2016) 8961951.
[87] S. Ohta, Curr. Pharm. Des. 17 (2011) 2241–2252.
[88] L. Yu, P. Hu, Y. Chen, et al., Adv. Mater. 30 (2018) 1801964.
[89] W. Fan, N. Lu, P. Huang, et al., Angew. Chem. Int. Ed. 56 (2017) 1229–1233.
[90] W. Fan, B.C. Yung, X. Chen, Angew. Chem. Int. Ed. 57 (2018) 8383–8394.
[91] M. Wang, Z. Hou, S. Liu, et al., Small 17 (2021) 2005728.
[92] Y. Zhou, W. Yu, J. Cao, et al., Biomaterials 255 (2020) 120193.
[93] J. Liu, R.S. Li, M. He, et al., Biomaterials 277 (2021) 121084.
[94] S. García-Gallego, G.J. Bernardes, Angew. Chem. Int. Ed. 53 (2014) 9712–9721.
[95] S.B. Wang, C. Zhang, Z.X. Chen, et al., ACS Nano 13 (2019) 5523–5532.
[96] Z. Meng, Y. Liu, Inhal. Toxicol. 19 (2007) 543–551.
[97] S. Li, R. Liu, X. Jiang, et al., ACS Nano 13 (2019) 2103–2113.
[98] M. Dole, F.R. Wilson, W.P. Fife, Science 190 (1975) 152–154.
[99] N.G. Milton, Drug. Aging 21 (2004) 81–100.
[100] R. Hu, C. Dai, C. Dong, et al., ACS Nano 16 (2022) 15959–15976.
[101] N. Kamimura, K. Nishimaki, I. Ohsawa, et al., Obesity 19 (2011) 1396–1403.
[102] P. Zhao, Z. Jin, Q. Chen, et al., Nat. Commun. 9 (2018) 4241.
[103] W. Pan, B. Cui, K. Wang, et al., Theranostics 11 (2021) 7869–7878.
[104] S.A. Lowndes, A. Adams, A. Timms, et al., Clin. Cancer Res. 14 (2008) 7526–7534.
[105] M. Finšgar, Corros. Sci. 77 (2013) 350–359.
[106] L.H. Fu, Z.Z. Wei, K.D. Hu, et al., J. Microbiol. 56 (2018) 238–245.
[107] F.J. Corpas, J.B. Barroso, S. González-Gordo, et al., J. Integr. Plant Biol. 61 (2019) 871–883.
[108] C. Xie, D. Cen, Z. Ren, et al., Adv. Sci. 7 (2020) 1903512.
[109] J.P. Kehrer, L.G. Lund, Free Radic. Biol. Med. 17 (1994) 65–75.
[110] T. Liu, L. Sun, Y. Zhang, et al., J. Biochem. Mol. Toxicol. 36 (2022) e22942.
[111] Y. Liu, J. Zhang, J. Du, et al., Acta Biomater. 129 (2021) 280–292.
[112] C.M. Grant, F.H. MacIver, I.W. Dawes, Mol. Biol. Cell 8 (1997) 1699–1707.
[113] L. Tian, M.M. Shi, H.J. Forman, Arch. Biochem. Biophys. 342 (1997) 126–133.
[114] B. Niu, K. Liao, Y. Zhou, et al., Biomaterials 277 (2021) 121110.
[115] R. Drew, J.O. Miners, Biochem. Pharmacol. 33 (1984) 2989–2994.
[116] Z. Huang, Y. Huang, M. Chen, et al., Chem. Eng. J. 399 (2020) 125667.
[117] J. Zhu, A. Jiao, Q. Li, et al., Acta Biomater. 137 (2022) 252–261.
[118] G. Chen, Y. Yang, Q. Xu, et al., Nano Lett. 20 (2020) 8141–8150.
[119] Y. Bian, B. Liu, S. Liang, et al., Chem. Eng. J. 435 (2022) 135046.
[120] M. Chang, M. Wang, M. Wang, et al., Adv. Mater. 31 (2019) 1905271.
[121] B. Ding, P. Zheng, F. Jiang, et al., Angew. Chem. Int. Ed. 59 (2020) 16381–16384.
[122] D. Qi, L. Xing, L. Shen, et al., Chin. Chem. Lett. 33 (2022) 4595–4599.
[123] H. Xiang, C. You, W. Liu, et al., Biomaterials 277 (2021) 121071.
[124] F. Wang, B. Wang, W. You, et al., Nano Res. 15 (2022) 9223–9233.
[125] F. Gong, L. Cheng, N. Yang, et al., Adv. Mater. 31 (2019) 1900730.
[126] Y. Dong, S. Dong, B. Liu, et al., Adv. Mater. 33 (2021) 2106838.
[127] B. Zhao, Y. Wang, X. Yao, et al., Nat. Commun. 12 (2021) 1345.
[128] T. Ruan, W. Liu, K. Tao, et al., Onco Targets Ther. 13 (2020) 1797.
[129] K. Bukowski, M. Kciuk, R. Kontek, Int. J. Mol. Sci. 21 (2020) 3233.
[130] J. Yan, Y. Zhang, L. Zheng, et al., Chin. Chem. Lett. 33 (2022) 767–772.
[131] S.K. Gupta, P. Singh, V. Ali, et al., Oncol. Rev. 14 (2020) 448.
[132] X. Cheng, D. Li, M. Sun, et al., Colloid Surf. B 181 (2019) 185–197.
[133] A.H. Schinkel, U. Mayer, E. Wagenaar, et al., Proc. Natl. Acad. Sci. U. S. A. 94 (1997) 4028–4033.
[134] H. Zhang, H. Xu, C.R. Ashby Jr, et al., Med. Res. Rev. 41 (2021) 525–555.
[135] C.P. Leith, K.J. Kopecky, I.M. Chen, et al., Blood 94 (1999) 1086–1099.
[136] S. Goto, T. Iida, S. Cho, et al., Free Radic. Res. 31 (1999) 549–558.
[137] G. Samimi, K. Katano, A.K. Holzer, et al., Mol. Pharmacol. 66 (2004) 25–32.
[138] H. Wang, Z. Gao, X. Liu, et al., Nat. Commun. 9 (2018) 562.
[139] X. Yao, S. Ma, S. Peng, et al., Adv. Healthc. Mater. 9 (2020) 1901582.
[140] M. Pljesa-Ercegovac, A. Savic-Radojevic, M. Matic, et al., Int. J. Mol. Sci. 19 (2018) 3785.
[141] B. Niu, Y. Zhou, K. Liao, et al., Acta Pharm. Sin. B 12 (2022) 2074–2088.
[142] H. Ge, J. Du, J. Zheng, et al., Chem. Eng. J. 446 (2022) 137040.
[143] J.K. Kang, J.C. Kim, Y. Shin, et al., Arch. Pharm. Res. 43 (2020) 46–57.
[144] M. Hou, Y. Zhong, L. Zhang, et al., Chin. Chem. Lett. 32 (2021) 1055–1060.
[145] A.R. Rastinehad, H. Anastos, E. Wajswol, et al., Proc. Natl. Acad. Sci. U. S. A. 116 (2019) 18590–18596.
[146] S.K. Sharma, N. Shrivastava, F. Rossi, et al., Nano Today 29 (2019) 100795.
[147] P.L. Moseley, J. Appl. Physiol. 83 (1997) 1413–1417.
[148] G. Gao, X. Sun, G. Liang, Adv. Funct. Mater. 31 (2021) 2100738.
[149] K. Yang, S. Zhao, B. Li, et al., Coord. Chem. Rev. 454 (2022) 214330.
[150] J. Zhou, M. Li, Y. Hou, et al., ACS Nano 12 (2018) 2858–2872.
[151] W. Ying, Y. Zhang, W. Gao, et al., ACS Nano 14 (2020) 9662–9674.
[152] M.M. Gaschler, B.R. Stockwell, Biochem. Biophys. Res. Commun. 482 (2017) 419–425.
[153] M. Chang, Z. Hou, M. Wang, et al., Angew. Chem. Int. Ed. 60 (2021) 12971–12979.
[154] D.W. Zheng, B. Li, C.X. Li, et al., Adv. Mater. 29 (2017) 1703822.
[155] X. Yao, B. Yang, C. Li, et al., Chem. Eng. J. 453 (2022) 139888.
[156] C. Li, Y. Wang, Y. Lu, et al., Chin. Chem. Lett. 31 (2020) 1183–1187.
[157] K. Ding, C. Zheng, L. Sun, Chin. Chem. Lett. 31 (2020) 1168–1172.
[158] B.P. Patel, U.M. Rawal, T.K. Dave, et al., Integr. Cancer Ther. 6 (2007) 365–372.
[159] B. Yang, Y. Chen, J. Shi, Chem. Rev. 119 (2019) 4881–4985.
[160] X. Zheng, J. Xie, X. Zhang, et al., Chin. Chem. Lett. 32 (2021) 243–257.
[161] H. Zhou, J. Ge, Q. Miao, et al., Bioconjugate Chem. 31 (2019) 315–331.